A New Class of Vitamin D Analogues that Induce Structural Rearrangement of the Ligand-Binding Pocket of the Receptor

Yuka Inaba,[†,‡] Nobuko Yoshimoto,[†] Yuta Sakamaki,[†,§] Makoto Nakabayashi,[‡,§] Teikichi Ikura,[‡] Hirokazu Tamamura,[§] Nobutoshi Ito,[‡] Masato Shimizu,[‡,§] and Keiko Yamamoto*[,†]

Laboratory of Drug Design and Medicinal Chemistry, Showa Pharmaceutical University, 3-3165 Higashi-Tamagawagakuen, Machida, Tokyo 194-8543, Japan, School of Biomedical Science, Institute of Biomaterials and Bioengineering, Tokyo Medical and Dental University, 2-3-10 Kanda-Surugadai, Chiyoda-ku, Tokyo 101-0062, Japan

Received November 13, 2008

To identify novel vitamin D receptor (VDR) ligands that induce a novel architecture within the ligand-binding pocket (LBP), we have investigated eight 22-butyl-1α,24-dihydroxyvitamin D_3 derivatives (**3**−**10**), all having a butyl group as the branched alkyl side chain. We found that the 22*S*-butyl-20-epi-25,26,27-trinorvitamin D derivative **5** was a potent VDR agonist, whereas the corresponding compound **4** with the natural configuration at C(20) was a potent VDR antagonist. Analogues with the full vitamin D_3 side chain were less potent agonist, and whether they were agonists or antagonists depended on the 24-configuration. X-ray crystal structures demonstrated that the VDR-LBD accommodating the potent agonist **5** has an architecture wherein the lower side and the helix 11 side of the LBP is simply expanded relative to the canonical active-VDR situation; in contrast, the potent antagonist **4** induces an extra cavity to accommodate the branched moiety. This is the first report of a VDR antagonist that generates a new cavity to alter the canonical pocket structure of the ligand occupied VDR.

Introduction

The hormonally active metabolite of vitamin D_3, 1α,25-dihydroxyvitamin D_3 [1,25-$(OH)_2D_3$, **1a**], plays an important role in calcium homeostasis, cell differentiation and proliferation, and immunomodulation.[1] 1,25-$(OH)_2D_3$ (**1a**) and its active analogues exert these effects by binding to the vitamin D receptor (VDR[a]), which belongs to the nuclear receptor superfamily.[2] The VDR is a ligand-dependent transcription factor that functions as a heterodimer with another nuclear receptor, retinoid X receptor (RXR).[3] Upon ligand binding, the VDR undergoes a conformational change that promotes RXR−VDR heterodimerization.[3] The RXR−VDR heterodimer binds to the vitamin D response elements present in the promoter region of responsive genes, recruits the coactivator, and initiates the transcription.

Since the first report of the X-ray crystal structure of the ligand binding domain (LBD) of the VDR complexed with the hormone 1,25-$(OH)_2D_3$ (**1a**) by Moras' group in 2000,[4] several groups have solved the crystal structures of the VDR−LBD complexed with a variety of ligands.[5−16] All of the crystal structures showed the canonical Moras' conformation of the VDR−LBD and quite similar architectures of the ligand binding pocket (LBP), except for the complex of zebrafish VDR−LBD with "GEMINI, **1b**",[7,11] an analogue with two identical side chains.[17,18] The zebrafish VDR−LBD/GEMINI complex revealed the formation of a new channel extending the original LBP in order to accommodate the second side chain. This particular observation suggests that the region around helix 6, the subsequent loop 6−7, and the N-terminal of helix 7 has a certain flexibility without loss of function because, despite the new pocket structure, GEMINI **1b** acts as a VDR agonist.[19] We considered that some new ligands having the right side chain might be able to change the induced pocket structure in such a way as to modulate the VDR differently. Here, we report a novel class of vitamin D analogues exhibiting a stereospecific dichotomy of activities.

Design and Synthesis

We have already reported that some 22-alkyl-1α,25-dihydroxyvitamin D_3, and in particular the 20-epi analogues, act as superagonists of the VDR.[20−22] Docking analysis and alanine scanning mutational analysis (ASMA) gave a clue that the 22-alkyl substituent of 22*R*-butyl-20-epi-1,25-$(OH)_2D_3$ **2** might induce a novel cavity in a similar way to GEMINI **1b**.[22] To explore further vitamin D compounds possessing a 22-butyl group, we have now investigated a series of 22-butyl-1α,24-dihydroxyvitamin D_3 derivatives **3**−**10** as candidate VDR modulators. The 25-to-24 transposition of the hydroxyl group is a known agonistic modification, notably seen in several clinically important vitamin D analogues. In compounds **3**−**6**, three carbons at the side chain terminus were removed to decrease the degree of hydrophobic interactions with helix 12, including the terminal of helix 11, of the VDR. On the basis of our previous study, we had concluded that insufficient hydrophobic interactions between the ligand and the C-terminal of the VDR cause antagonistic behavior.[23] Compounds **7**−**10** were designed as the counterparts of side chain truncated analogues **3** and **4** to test the significance of the hydrophobic interactions (Chart 1).

As shown in Scheme 1, 22-butyl vitamin D derivatives **3** and **4** were synthesized from 22*R*-butyl compound **11** and 22*S*-butyl compound **12**, respectively, which are the established products of a diastereofacial selective conjugate addition reaction of *n*-Bu_2CuLi with the *E*- and *Z*-enoates developed by our group previously.[24] The configuration at C(22) follows from the

* To whom correspondence should be addressed. Phone: +81 42 721 1580. Fax: +81 42 721 1580. E-mail: yamamoto@ac.shoyaku.ac.jp.

† Laboratory of Drug Design and Medicinal Chemistry, Showa Pharmaceutical University.

‡ School of Biomedical Science, Tokyo Medical and Dental University.

§ Institute of Biomaterials and Bioengineering, Tokyo Medical and Dental University.

[a] Abbreviations: VDR, vitamin D receptor; LBP, ligand binding pocket; 1,25-$(OH)_2D_3$, 1α,25-dihydroxyvitamin D_3; RXR, retinoid X receptor; LBD, ligand binding domain; ASMA, alanine scanning mutational analysis.

10.1021/jm8014348 CCC: $40.75
Published on Web 02/04/2009

Chart 1. Structures of 1,25-$(OH)_2D_3$ (**1a**) and Its Derivatives

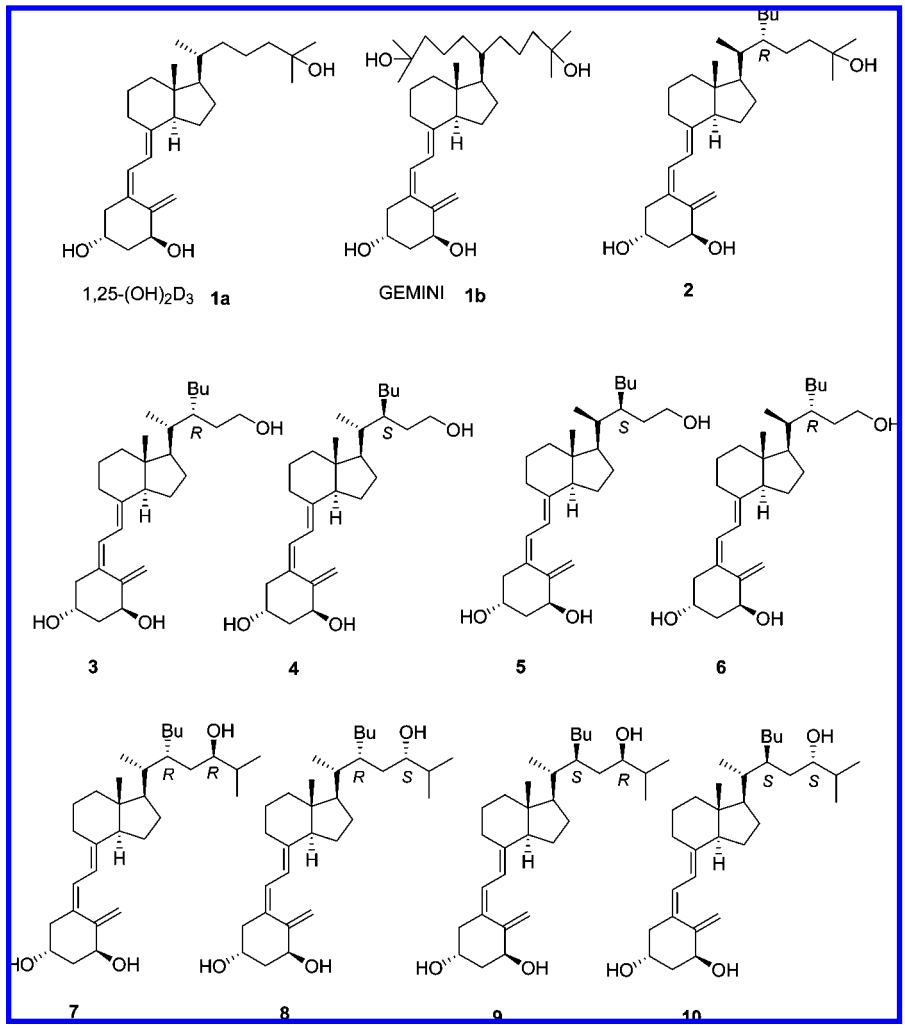

stereochemistry of the starting enoates and the reaction conditions.[24] Reduction of the side chain ester together with reductive cleavage of the carbonates at C(1) and C(3) as protecting groups of **11** and **12** gave provitamins D, **13** and **14**, respectively. These provitamins were converted to the desired vitamin D analogues **3** and **4** by the biomimetic sequence of photoirradiation with a high-pressure mercury lamp, followed by thermal isomerization. The 20-epi-analogues **5** and **6** were synthesized by the analogous procedure as that described above for the synthesis of the 20-normal analogues **3** and **4**.

22-Butyl-1α,24-dihydroxyvitamins D_3 **7**−**10** were successfully synthesized from the same 22-butyl compounds **11** and **12**. Controlled chemoselective reduction of the methyl esters of **11** and **12** by DIBAL afforded 24-alcohols **19** and **20**, respectively. Swern oxidation of the 24-alcohols **19** and **20** gave the aldehyde **21** and **22**, respectively. 22*R*-aldehyde **21** reacted with *i*-PrMgCl to give the 24*R*- and 24*S*-isomers **23** (less polar) and **24** (more polar), while 22*S*-aldehyde **22** reacted with *i*-PrMgCl to give the 24*R*- and 24*S*-isomers **25** (less polar) and **26** (more polar). Epimers were separated by column chromatography. The configuration at C24 was determined by the Kusumi−Mosher method (Scheme 2).[25] Thus, less polar compound **23** was converted to the corresponding *S*- and *R*-MTPA esters of the 24-hydroxyl group (**31** and **32**), and the 22-isomer **26** was also converted to those of the 24-hydroxyl group (**33** and **34**). Chemical shift differences between the *S*-MTPA ester and the corresponding *R*-MTPA ester are shown in Figure 1a,b. This analysis clearly indicated that the 24-alcohols **23** and **26** have a 24*R*-configuration and a 24*S*-configuration, respectively. Consequently, the configurations of 24-isomers **24** and **25** were demonstrated to be *S* and *R*, respectively. Methyl carbonates at C(1) and C(3) were saponified to give provitamins D **27**−**30**. These provitamins were converted to the desired vitamin D analogues **7**−**10** by photoirradiation, followed by thermal isomerization.

Biological Activities

Binding affinity for the VDR was evaluated by the standard competitive binding assay using bovine thymus VDR, which has a LBD amino acid sequence[26] identical to that of the human VDR.[27] The results are summarized in Table 1. Of the four 22-butyl-1α,24-dihydroxy-25,26,27-trinorvitamins D_3 **3**−**6**, the 22*S*-compounds **4** and **5** showed significant affinity compared to the natural hormone **1a**, while their 22*R*-isomers **3** and **6** showed weak affinity for the VDR. Among the four 22-butyl-1α,24-dihydroxyvitamins D_3 **7**−**10**, both of the 24*S*-hydroxyl compounds **8** and **10** showed significant affinity for the VDR, while both the 24*R*-hydroxyl compounds **7** and **9** showed relatively weak affinity.

The ability of 22-butyl compounds **3**−**10** to induce transcription of a vitamin D-responsive gene was tested using the rat osteopontin luciferase reporter gene assay system in Cos7 cells, and the results are shown in Figure 2. In this assay, only

Scheme 1. Synthetic Sequence Leading to Target Compounds **3**−**10**

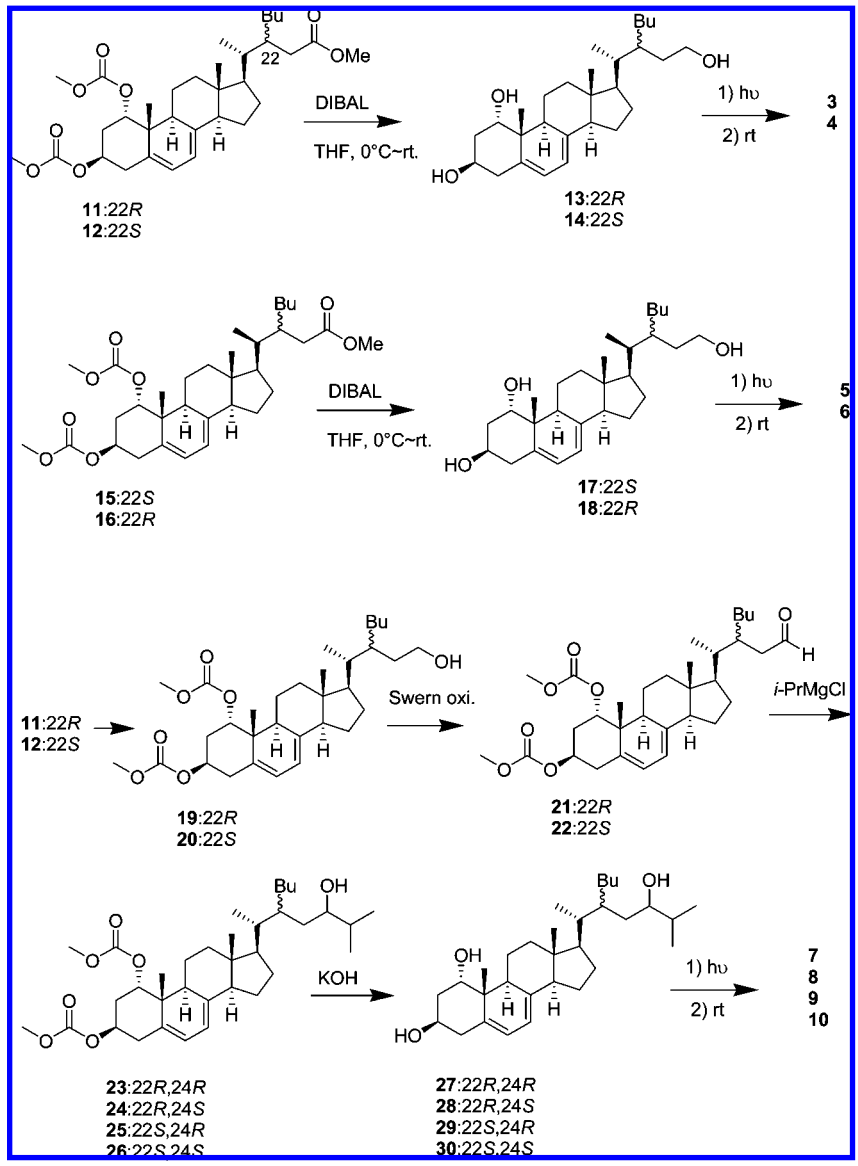

Scheme 2. MTPA esters from 24-Alcohols **23** and **26**

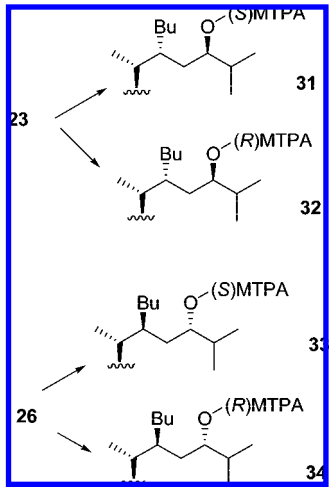

compound **5** showed full agonistic activity and two analogues **7** and **9** showed weak agonist activity. All of the others, **3**, **4**, **6**, **8**, and **10**, showed little activity. It is known that receptor affinity and transactivation potency are not proportional to each other.[22,28] The potency to inhibit VDR activation was evaluated in the presence of 1 nM 1,25-$(OH)_2D_3$ (**1a**). As shown in Figure 2, compounds **4**, **6**, **8**, and **10** concentration-dependently inhibited the transactivation induced by 1,25-$(OH)_2D_3$ (**1a**), indicating that these four analogues work as VDR antagonists. We performed the same assays in HEK293 cells and obtained similar results (see Supporting Information Figure S1).

We evaluated the expression of CYP24A1 mRNA in HEK293 cells by quantitative real-time PCR. CYP24A1 is known to be the most potent target gene of the hormone 1,25-$(OH)_2D_3$ (**1**).[29a] In accordance with the transcriptional activities of our synthetic ligands described above, only compound **5** expressed CYP24A1 mRNA strongly in comparison with the natural hormone **1a**, and compound **9** showed weak expression activity (Figure 3a,b). All of the others, **3**, **4**, **6**, **7**, **8**, and **10**, showed little activity. The inhibition potency of synthetic ligands for CYP24A1 mRNA expression was evaluated in the presence of 10 nM 1,25-$(OH)_2D_3$ (**1a**). As shown in Figure 3a,b, compounds **4**, **6**, **8**, and **10** significantly inhibited the gene expression induced by 1,25-$(OH)_2D_3$ (**1a**). Figure 3c shows that compound **4** inhibited the gene expression concentration-dependently.

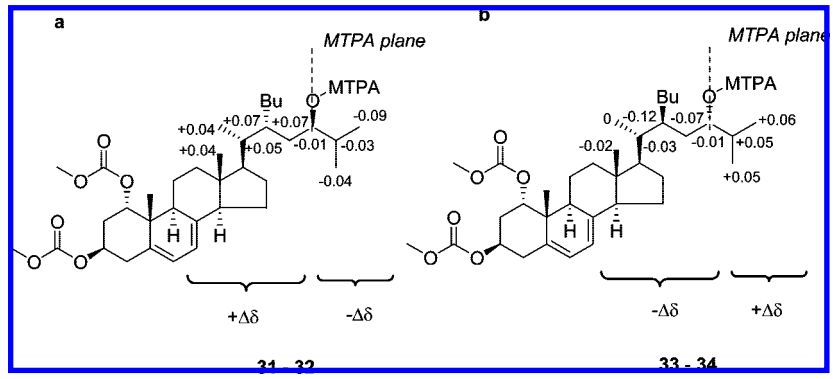

Figure 1. Determination of stereochemistry at C(24). Chemical shift differences.

Table 1. VDR Binding Affinity of 22-Butyl Compounds **3**−**10**[a]

	1a	**3** (22*R*)	**4** (22*S*)	**5** (22*S*)	**6** (22*R*)	**7** (22*R*,24*R*)	**8** (22*R*,24*S*)	**9** (22*S*,24*R*)	**10** (22*S*,24*S*)
EC_{50} (nM)[b]	0.05	11	1.2	2.0	20	16	3.4	20	3.8
relative affinity[c]	1	1/220	1/24	1/40	1/400	1/320	1/68	1/400	1/76

[a] Competitive binding of 1,25-$(OH)_2D_3$ (**1a**) and 22-butyl compounds (**3**−**10**) to the bovine thymus vitamin D receptor. The experiments were carried out in duplicate. [b] The EC_{50} values are derived from dose−response curves and represent the compound concentration required for 50% displacement of the radio-labeled 1,25-$(OH)_2D_3$ from the receptor protein. [c] Affinity relative to 1,25-$(OH)_2D_3$ (**1a**), the activity of **1a** being defined as 1.

Cell differentiation and antiproliferation activity were evaluated using human promyelocyte HL-60 cells.[29b] Compound **5** showed significant activity for differentiation of HL-60 cells into monocytes/macrophages (Figure 4), being comparable to that of 1,25-$(OH)_2D_3$ (**1a**), whereas compound **9** showed weak activity. None of the other compounds induced differentiation of HL-60 cells. Similar results were obtained in experiments examining the antiproliferative effect on HL-60 cells (data not shown). Ligand **4** concentration-dependently inhibited the differentiation and antiproliferation of HL-60 cells induced by stimulation with 1,25-$(OH)_2D_3$ (**1a**) (Figure 4c). Morphologic analysis also indicated that the differentiation of HL-60 cells was inhibited by ligand **4** (Figure 4d).

Thus, in all assays, ligands **4** and **5** were demonstrated to behave as a potent antagonist and a potent agonist, respectively.

Alanine Scanning Mutational Analysis

We have developed and reported a method for exhaustive alanine scanning mutational analysis (ASMA) of residues lining the LBP of the VDR.[30] We applied this analysis to all eight compounds **3**−**10**. Transactivation was examined using 22-butyl compounds (**3**−**10**) at a concentration of 10^{-6} M. The results are shown in Figure S2 (see Supporting Information) in comparison with the natural hormone (**1a**) and the parent molecule, 22*R*-butyl-20-epi-1,25-$(OH)_2D_3$ **2**.

Recruitment of RXR and Coactivator Peptide

We evaluated ligand-dependent recruitment of the RXR and a coactivator peptide, SRC-1, to the VDR using a mammalian two-hybrid assay similar to that reported previously.[31] As shown in Figure S3 of the Supporting Information, compound **5** recruited the RXR and SRC-1 strongly, whereas compounds **7** and **9** did so weakly. Inhibition of SRC-1 recruitment induced by natural hormone **1a** was observed for compounds **4**, **8**, and **10** (data not shown).

Structure

To understand the molecular basis of action of our synthetic ligands, we conducted X-ray crystal structure analysis of the VDR−LBD/ligand complex and successfully solved the crystal structure of rat VDR−LBD bound to the potent agonist **5** in the presence of the coactivator peptide at 2.1 Å resolution (Table 2). A ribbon-tube representation of the rVDR−LBD/**5**/peptide complex is shown in Figure 5a, and the results of the crystallographic refinement are summarized in Table 2. The electron density of the VDR−LBD complex including ligand **5** is well defined. The overall structure of the VDR−LBD is similar to that observed for VDR−LBD bound to 1,25-$(OH)_2D_3$ (**1a**),[15] although the ligand **5** has a branched alkyl side chain. The coactivator peptide is tightly bound to the activation function 2 surface formed by helices 3, 4, and 12 of the LBD and occupies the typical agonist position (Figure 5a). However, the docking mode of agonist **5** is unusual. In the crystal structure, the part from the A-ring to the D-ring occupies almost the same position as that of 1,25-$(OH)_2D_3$ (**1a**), but the mode in which the side chain is accommodated into the pocket is unique (Figure 5b), i.e., the 22-butyl group, and not the canonical side chain bearing the 24-hydroxyl group, is oriented toward helix 12, and the 24-hydroxyl group itself is oriented toward helix 6 to form a hydrogen bond with the carbonyl oxygen of the main chain of Val296 (hVal300) on helix 6. Because both of the side chains of ligand **5** are accommodated tightly in the pocket of the VDR active conformation, the pocket is slightly expanded in the bottom (lower) region, where the side chain hydroxyl group of **5** is located, and in the terminal region of helix 11, where the terminal of the butyl group of **5** is located together with a molecule. The expansion of the bottom region results from steric repulsion between the side chains of the residues on helix 6 and the subsequent loop 6−7 of the VDR and the 24-hydroxyl group of ligand **5**. Expansion at the helix 11 side is caused by twisting of the side chain of Leu400 (hLeu404) on loop 11−12 (Figure 5b).

To understand the structural basis of the antagonistic effect of compound **4**, we attempted to solve the crystal structure of the VDR−LBD/**4** complex. We were able to obtain crystals of the complex in the presence of the coactivator peptide, but not in its absence. The resolution of the ternary complex (rVDR−LBD/**4**/peptide) was 3.0 Å (Table 2). The electron density of the main chain of the VDR−LBD and almost all of ligand **4** was clearly observed. The overall structure of the main chain, including helices 11 and 12, is quite similar to that of the VDR−LBD/**1a**/peptide complex (Figure 6a). The main chains of only two

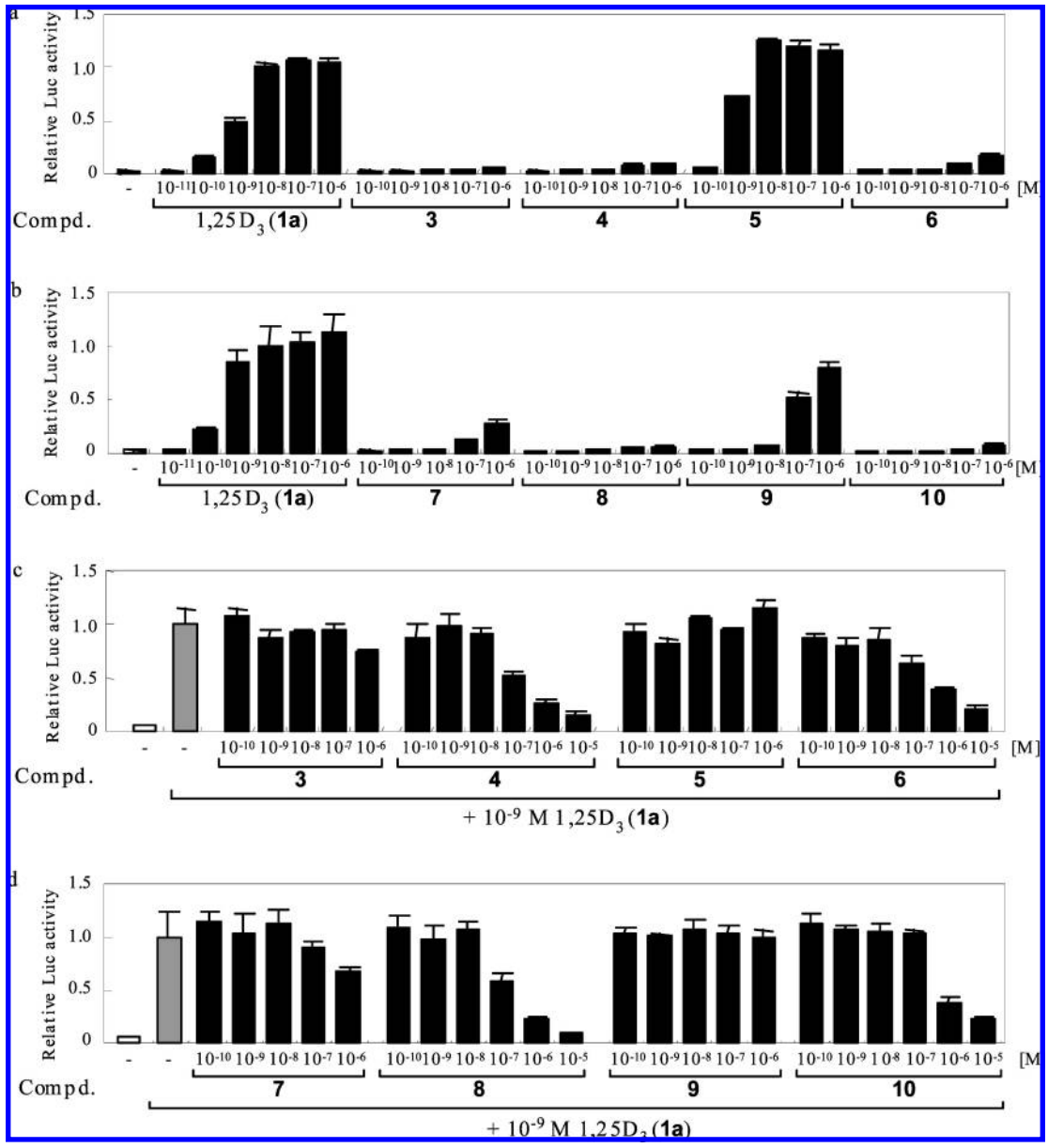

Figure 2. Transactivation of compounds **3**−**10** in Cos7 cells. Transcriptional activity (a and b) and inhibitory effect on the transactivation induced by 1,25-$(OH)_2D_3$ (**1a**) (c and d) were evaluated by dual luciferase assay using a full-length human VDR expression plasmid (pCMX-hVDR), a reporter plasmid containing three copies of the mouse osteopontin VDRE (SPPx3-TK-Luc), and the internal control plasmid containing sea pansy luciferase expression constructs (pRL-CMV) in Cos7 cells as described previously.[32] Luciferase activity in the presence of 10^{-8} M 1,25-$(OH)_2D_3$ (**1a**) was defined as 1: (a) transcriptional activity of **1a** and **3**−**6**, (b) transcriptional activity of **1a** and **7**−**10**, (c) transcriptional activity of **3**−**6** in the presence of 10^{-9} M 1,25-$(OH)_2D_3$ (**1a**), (d) transcriptional activity of **7**−**10** in the presence of 10^{-9} M 1,25-$(OH)_2D_3$ (**1a**). All experiments were done in triplicate.

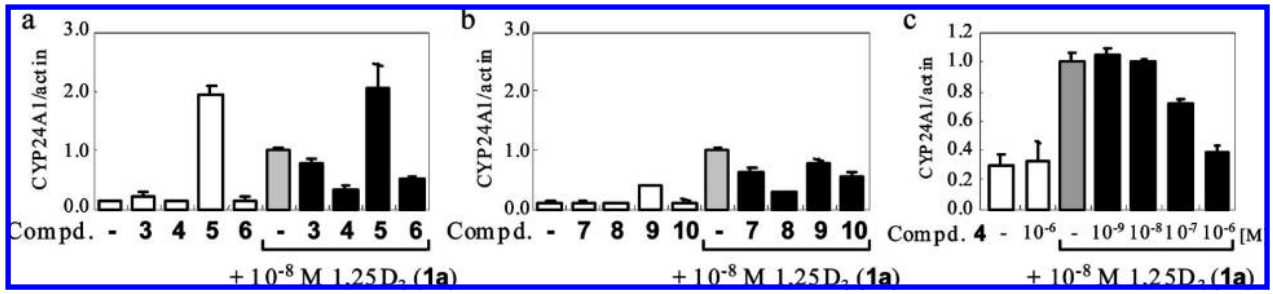

Figure 3. Effect of **1a** and 22-butyl compounds (**3**−**10**) on expression of the CYP24A1 gene in HEK293 cells. (a,b) Cells were treated with 10^{-6} M 22-butyl compounds ((a) **3**−**6**, (b) **7**−**10**) in the absence or presence of 10^{-8} M 1,25-$(OH)_2D_3$ (**1a**) for 24 h. Concentration (10^{-6} M) of test compounds was selected to obtain clear results concerning whether they activate CYP24A1 expression or inhibit it. (c) Cells were treated with the indicated concentrations of compounds for 24 h. All experiments were carried out in triplicate.

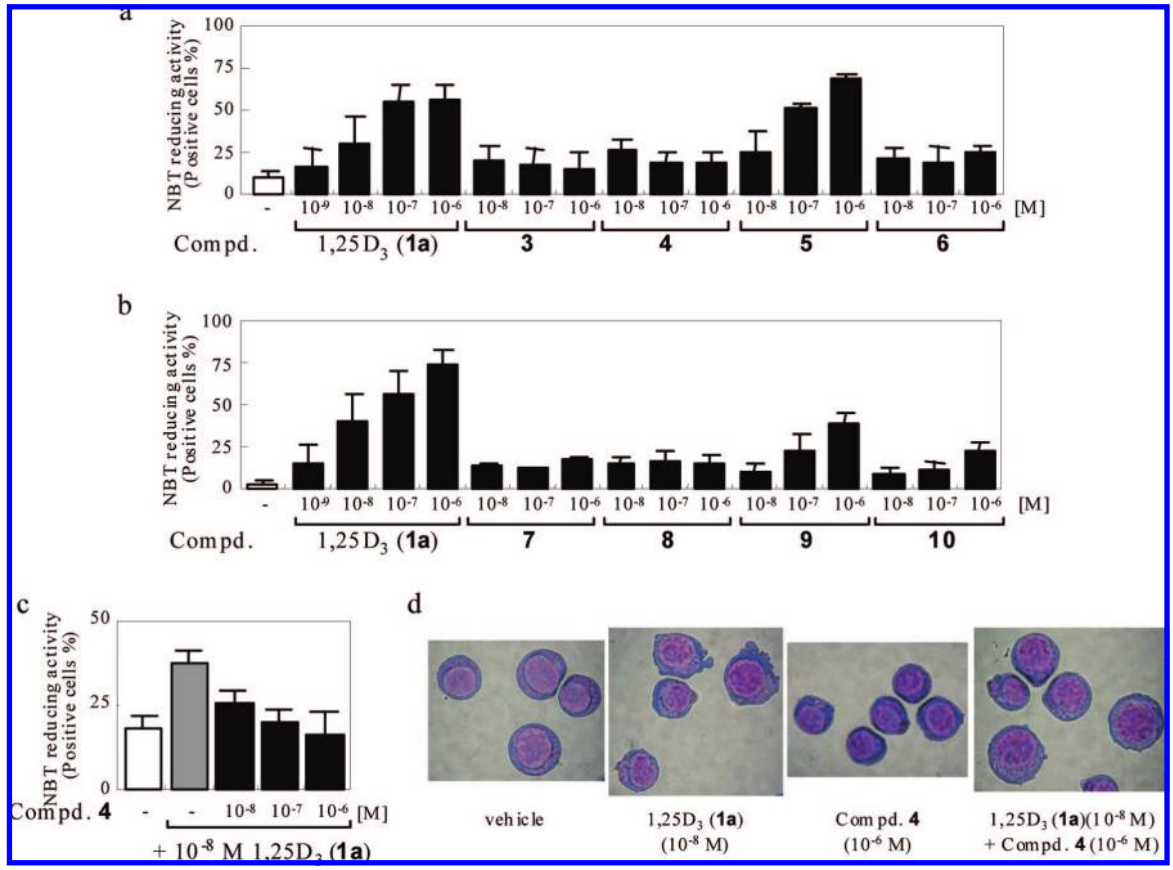

Figure 4. Effect of **1a** and 22-butyl compounds (**3**−**10**) on differentiation of HL-60 cells. (a−c) Cells were treated with the indicated concentrations of compounds for four days. Differentiation was determined by nitro blue tetrazolium (NBT) reduction.[33] All experiments were carried out in triplicate. (d) HL-60 cells were stained with Wright−Giemsa and analyzed for morphology by light microscopy.

Table 2. Summary of Data Collection Statistics and Refinement

ligand	compd **4**	compd **5**
X-ray source	KEK-PF BL-6A	KEK-PF BL-6A
wavelength (Å)	0.97800	0.97800
space group	*C*2	*C*2
unit cell dimensions (Å)	$a = 153.25$, $b = 43.42$, $c = 42.37$	$a = 153.16$, $b = 43.88$, $c = 41.89$
(deg)	$\alpha = 90.00$, $\beta = 95.97$, $\gamma = 90.00$	$\alpha = 90.00$, $\beta = 95.89$, $\gamma = 90.00$
resolution range (Å)[a]	50.00−3.00 (3.11−3.00)	50.00−2.10 (2.18−2.10)
total number of reflections	17932	59861
no. of unique reflections	5664	16470
% completeness[a]	99.1 (99.8)	97.5 (92.2)
R_{merge}[a,b]	0.086 (0.392)	0.045 (0.234)
refinement statistics		
resolution range (Å)[a]	50.00−3.00 (3.11−3.00)	50.00−2.10 (2.18−2.10)
R factor (R_{free}/R_{work})[a,c]	0.295 (0.431)/0.226 (0.321)	0.251 (0.367)/0.209 (0.336)

[a] Values in parentheses are for the highest-resolution shell. [b] $R_{merge} = \sum|(I_{hkl} - \langle I_{hkl}\rangle)|/(\sum I_{hkl})$, where $\langle I_{hkl}\rangle$ is the mean intensity of all reflections equivalent to reflection *hkl*. [c] R_{work} (R_{free}) $= \sum||F_{obs}| - |F_{calc}||/\sum|F_{obs}|$, where 10% of randomly selected data were used for R_{free}.

amino acid residues, Leu305 (hLeu309) and Ser394 (hSer398), are slightly twisted outward (Figure 6b). The crystal structure clearly demonstrated that a novel cavity is produced in the region surrounded by helix 6, the subsequent loop 6−7, the N-terminal of helix 7 and helix 11, as in the zVDR/GEMINI complex, because the terminal of the 22-butyl group of **4** pushes out the side chain of Leu305 to rearrange the LBP (Figure 6c,d).

Thus, we identified a new class of VDR ligands with a simple side chain that modulate the structure of the LBP.

Discussion

Compound **5** was proved to have potent agonistic activity by additional experiments involving RXR recruitment and SRC-1 peptide recruitment using a mammalian two-hybrid assay (see Supporting Information Figure S3). These experimental results corroborate the crystal structure of the VDR−LBD/**5**/peptide complex (Figure 5). Thus, the overall surface structure is rather similar to that of the VDR−LBD/**1a**/peptide complex. On the other hand, ligand **5** is accommodated into the LBP by an unusual docking mode in which two side chains of ligand **5**, together with a molecule, increase the volume of the LBP. The pocket is filled sufficiently with ligand **5** and a water molecule. These observations well account for the potent activity of compound **5**.

The antagonistic activity of compound **4** was also confirmed by experiments involving RXR recruitment and SRC-1 peptide recruitment (see Supporting Information Figure S3). So far, the X-ray crystal structure of the VDR−LBD/antagonist complex, which clearly explains the structural basis of the antagonism,

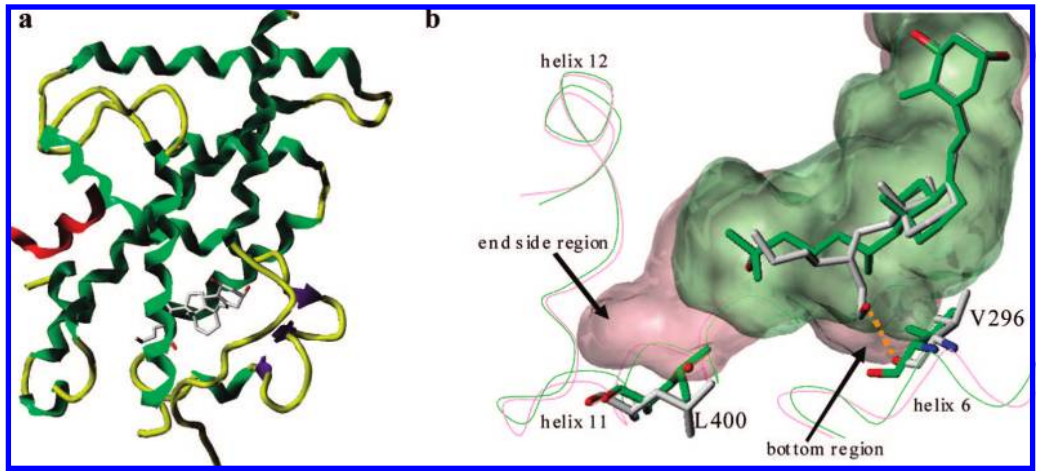

Figure 5. X-ray crystal structure of rVDR−LBD/**5**/peptide complex. (a) Overall view of rVDR−LBD/**5**/peptide complex. Helices, loops, β-sheets, and coactivator peptide are shown in green, yellow, violet, and red, respectively. Ligand **5** is shown in gray with the oxygen atoms in red. (b) Superposition of rVDR−LBD/**1a**/peptide (green) and rVDR−LBD/**5**/peptide (pink) in the ligand binding pocket (LBP) region. Connolly channel surfaces of the LBP of rVDR−LBD/**1a**/peptide and rVDR−LBD/**5**/peptide are shown in green and pink, respectively. Hydrogen bond is shown with dotted orange line. Water molecule is shown in red sphere.

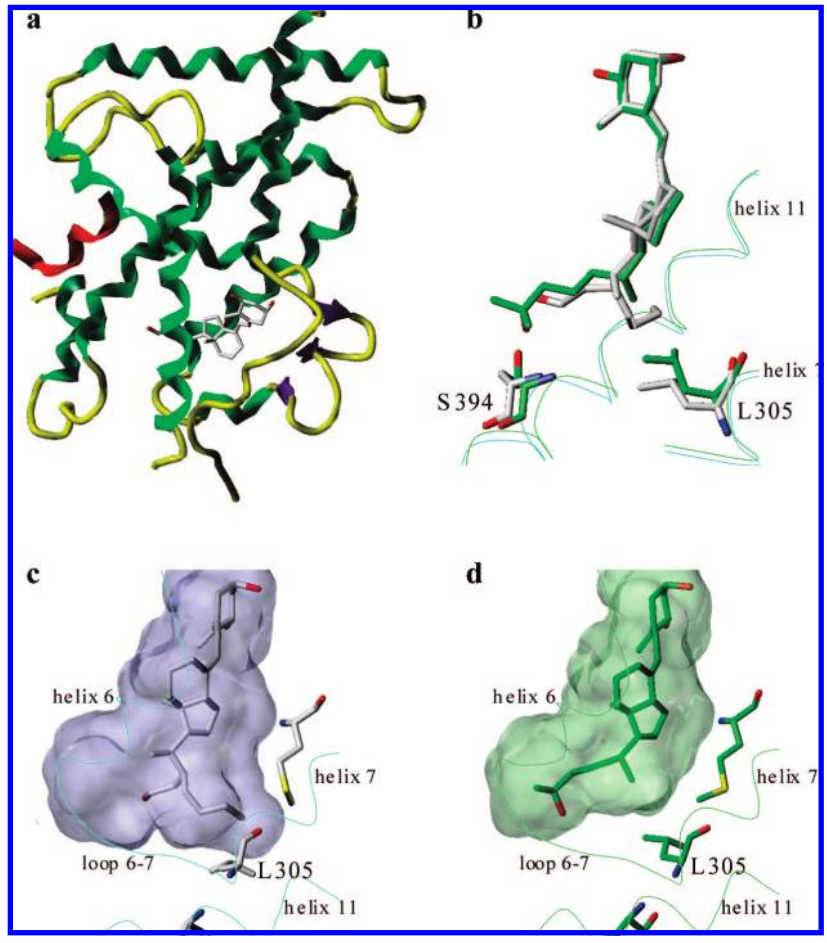

Figure 6. X-ray crystal structure of rVDR−LBD/**4**/peptide complex. (a) Overall view of rVDR−LBD/**4**/peptide complex. Helices, loops, β-sheets, and coactivator peptide are shown in green, yellow, violet, and red, respectively. The ligand **4** is shown in gray with the oxygen atoms in red. (b) Superposition of rVDR−LBD/**1a**/peptide (green) and rVDR−LBD/**4**/peptide (gray) in the ligand biding pocket (LBP) region. (c) Connolly channel surface of the LBP of rVDR−LBD/**4**/peptide. (d) Connolly channel surface of the LBP of rVDR−LBD/**1a**/peptide.

has not been reported. Quite recently, the crystal structure of the VDR−LBD complex accommodating an antagonist with a coactivator peptide was reported, where the ligand was bound to the active (agonistic) conformation of the VDR.[16] This situation was also the case in the present study. We were able to obtain crystals of the VDR−LBD/**4** complex in the presence of, but not in the absence of, the coactivator peptide as a ternary complex (Figure 6). Considering the action of compound **4** as a VDR antagonist, the active (agonistic) conformation of the VDR−LBD/**4** complex bound tightly to the peptide seems to be a temporary and less preferred structure but selected in the course of crystallization. This idea is consistent with the fact

that the resolution limit of this crystal (3.0 Å) is much lower than that of the crystal for compound **5** (2.1 Å). Therefore, the active conformation observed in our crystal structure may not exactly correspond to the predominant one in vivo. Meanwhile, it is true that ligand **4** modifies the pocket structure to induce a new cavity, as seen in the zVDR−LBD/GEMINI complex.[11] Unlike GEMINI, however, compound **4** showed antagonistic activity. This discrimination can be explained mainly by the difference in hydrophobic interactions between the side chain terminals of the ligand and the C-terminal of the VDR. This explanation agrees with the fact that compound **9**, which restored the three truncated carbons on the side chain, restored the agonistic activity, albeit weakly.

Compound **6**, which is 25,26,27-trinor analogue of the previously reported 22*R*-butyl-20-epi-1,25-$(OH)_2D_3$ **2**, having potent agonistic activity,[22] showed weak VDR affinity and little agonistic or antagonistic activity. ASMA of compound **6** yielded results similar to those for 22*R*-butyl-20-epi-1,25-$(OH)_2D_3$ **2**, indicating that **6** is accommodated into the VDR−LBD by the similar docking mode to that of the parent compound **2**. However, interaction of a hydrogen bond with His397 is not important for **6** because H397A did not decrease the transcriptional activity in comparison with the wild type. In addition, compound **6** lacks the intimate hydrophobic interactions with the C-terminal residues of the VDR because of truncation of the three carbons in the side chain terminal. Therefore, the weak activity of ligand **6** is attributable to poor interaction with the C-terminal regions (helix 11-helix 12) of the VDR.

Docking analysis of ligand **8** into the crystal structure of the VDR−LBD/**4**/peptide complex demonstrated that the two side chains of ligand **8** occupy opposite cavities, respectively, (data not shown) in comparison with the VDR−LBD/**4** complex. This mode is consistent with the results of ASMA. The increased activity of H397A and H305A compared with the wild type (Supporting Information Figure S2h) suggests that His397 does not form an important hydrogen bond with ligand **8** and His305 exhibits crucial steric repulsion from the ligand.

Docking analysis of ligand **10** demonstrated that its mode of docking into the LBP is similar to that of compound **4**. When taking together with the results of ASMA, it appears that steric repulsion between the *i*-propyl group of the side chain terminal of **10** and the side chain of His305 explains the antagonistic activity.

GEMINI (**1b**), which has two identical side chains branching at C(20), induces structural rearrangement of the LBP.[11] We identified potent agonist **5** and potent antagonist **4**, both of which have a branched 22*S*-butyl group and are isomers at C(20). We found that both ligands rearrange the pocket structure of the VDR through an unusual docking mode that has not yet been reported. Other ligands (**3**, **6**−**10**) showed intermediate activities (weakly agonistic and weakly antagonistic) and appeared to modify the LBP structure moderately. It is interesting that although GEMINI (**1b**) and our compound **4** are accommodated into the VDR−LBD through a similar docking mode, GEMINI (**1b**) works as a VDR agonist whereas compound **4** works as a VDR antagonist.

Conclusions

We synthesized 22-butyl-1,24-$(OH)_2D_3$ derivatives **3**−**10** and evaluated their biological activities. Four compounds, **4**, **5**, **8**, and **10**, showed significant VDR binding affinity but three of them, **4**, **8**, and **10**, showed little transactivation, cell differentiation, and CYP24A1 gene expression potency. Instead, these three compounds concentration-dependently inhibited biological activities induced by 1,25-$(OH)_2D_3$, indicating that they are VDR antagonists. On the basis of X-ray crystallographic analysis, we identified a new class of ligands that modulate the pocket structure of the VDR. This is the first report of a VDR antagonist that generates a new cavity to alter the pocket structure of the VDR, opening an interesting new perspective of ligand design based on the alternative structural basis of VDR agonism and antagonism.

Experimental Section

^{1}H NMR and ^{13}C NMR spectra were recorded in $CDCl_3$ at 400 MHz, and chemical shifts are reported as δ units relative to tetramethylsilane as an internal standard. High and low resolution mass spectra were obtained at 70 eV. Relative intensities are given in parentheses in low mass. IR spectra were recorded on a Shimazu FTIR spectrometer. UV spectra were recorded on a BECKMAN DU7500 spectrophotometer. All air and moisture sensitive reactions were carried out under argon atmosphere.

22*R*-Butyl-(1α,3β)-chola-5,7-diene-1,3,24-triol (13). To a solution of **11** (50 mg, 0.087 mmol) in THF (1 mL) was added diisobutyl-alminum hydride (DIBAL, 1.0 M solution in toluene, 1000 μL, 1 mmol) at 0 °C and the mixture was stirred for 2.5 h. Then the mixture was allowed to come to room temperature and was stirred for 10 h. The reaction mixture was poured into ice−water, extracted with ethyl acetate, washed with water, dried over Na_2SO_4, and evaporated. The residue was chromatographed on silica gel (C-200, 4 g) with 3% EtOH−CH_2Cl_2 to give **13** (24 mg, 64%). ^{1}H NMR δ 0.64 (3 H, s, H-18), 0.81 (3 H, d, J = 6.9 Hz, H-21), 0.90 (3 H, t, J = 6.4 Hz, *CH*$_3$ of *n*-Bu), 0.95 (3 H, s, H-19), 3.58 and 3.71 (each 1 H, m, H-24), 3.77 (1 H, m, H-1), 4.08 (1 H, m, H-3), 5.38 and 5.74 (each 1 H, m, H-6 and H-7). MS *m*/*z* 430 (M^+, 10), 412 (6), 394 (11), 371 (13), 55 (100). UV (EtOH) λ_{max} 272, 282, 294 nm.

22*S*-Butyl-(1α,3β)-chola-5,7-diene-1,3,24-triol (14). The compound **14** was obtained from **12** (0.35 mmol) by the same procedure as described for **13** (yield 75%). ^{1}H NMR δ 0.63 (3 H, s, H-18), 0.83 (3 H, d, J = 6.1 Hz, H-21), 0.90 (3 H, t, J = 6.7 Hz, *CH*$_3$ of Bu), 0.95 (3 H, s, H-19), 3.62 and 3.68 (each 1 H, m, H-24), 3.77 (1 H, m, H-1), 4.07 (1 H, m, H-3), 5.38 and 5.74 (each 1 H, m, H-6 and H-7). MS *m*/*z* 430 (M^+, 14), 412 (8), 394 (15), 371 (20), 55 (100). UV (EtOH) λ_{max} 272, 282, 294 nm.

22*R*-Butyl-1α,24-dihydroxy-24,25,26-trinorvitamin D_3 (3). A solution of provitamin D **13** (22 mg, 0.051 mmol) in benzene/EtOH (130:50, 180 mL) was bubbled with argon at 0 °C for 15 min and then irradiated with a 100 W high pressure mercury lamp through a Vycor filter until most of the starting material **13** was consumed. After removal of the solvent, the residue was chromatographed on Sephadex LH-20 (15 g) with $CHCl_3$/hexane/MeOH (70:30:1.5) to give previtamin D. The previtamin D in 95% EtOH (5 mL) was stored in the dark at room temperature. After 12 days, the solution was evaporated and the residue was chromatographed on Sephadex LH-20 (15 g) with $CHCl_3$/hexane/MeOH (70:30:2) to give desired vitamin D **3** (5.0 mg, 23%). The purity was proved to be more than 99% by two different HPLC systems: (1) YMC Pack ODS-AM 4.6 mm × 150 mm, H_2O/MeOH (15:85), 1.0 mL/min; (2) PEGASIL Silica SP100, 4.6 mm × 150 mm, hexane/$CHCl_3$/MeOH (100:25:10), 1.0 mL/min. ^{1}H NMR δ 0.56 (3 H, s, H-18), 0.79 (3 H, d, J = 6.7 Hz, H-21), 0.89 (3 H, t, J = 6.7 Hz, *CH*$_3$ of *n*-Bu), 3.58 and 3.72 (each 1 H, m, H-24), 4.23 (1 H, m, H-3), 4.43 (1 H, m, H-1), 5.00 and 5.33 (each 1 H, s, H-19), 6.02 and 6.38 (each 1 H, d, J = 11.0 Hz, H-7 and H-6, respectively). MS *m*/*z* 430 (M^+, 3), 412 (7), 394 (5), 371 (2),134 (87), 55 (100). UV (EtOH) λ_{max} 263 nm, λ_{min} 228 nm. HRMS calcd for $C_{28}H_{46}O_3$ 430.3447, found 430.3436.

22*S*-Butyl-1α,24-dihydroxy-24,25,26-trinorvitamin D_3 (4). The compound **4** was obtained from **14** (0.022 mmol) by the same procedure as described for **3** (yield 26%). The purity was proved to be more than 99% by two different HPLC systems: (1) YMC Pack ODS-AM 4.6 mm × 150 mm, H_2O/MeOH (15:85), 1.0 mL/min; (2) PEGASIL Silica SP100, 4.6 mm × 150 mm, hexane/$CHCl_3$/MeOH (100:25:10), 1.0 mL/min. ^{1}H NMR δ 0.55 (3 H, s,

H-18), 0.81 (3 H, d, $J = 6.7$ Hz, H-21), 0.90 (3 H, t, $J = 7.4$ Hz, *CH*$_3$ of Bu), 3.62 and 3.66 (each 1 H, m, H-24), 4.23 (1 H, m, H-3), 4.43 (1 H, m, H-1), 5.00 and 5.33 (each 1 H, m, H-19), 6.02 and 6.38 (each 1 H, d, $J = 11.0$ Hz, H-7 and H-6, respectively). MS *m*/*z* 430 (M^+, 4), 412 (7), 394 (5), 371 (2),134 (65), 55 (100). UV (EtOH) λ_{max} 264 nm, λ_{min} 228 nm. HRMS calcd for $C_{28}H_{46}O_3$ 430.3447, found 430.3438.

20*S*,22*R*-Butyl-(1α,3*β*)-chola-5,7-diene-1,3,24-triol (18). The compound **18** was obtained from **16** (0.08 mmol) by the same procedure as described for **13** (yield 62%). ^{1}H NMR δ 0.63 (3 H, s, H-18), 0.74 (3 H, d, $J = 6.1$ Hz, H-21), 0.90 (3 H, t, $J = 6.7$ Hz, *CH*$_3$ of Bu), 0.94 (3 H, s, H-19), 3.68 (2 H, m, H-24), 3.77 (1 H, m, H-1), 4.06 (1 H, m, H-3), 5.38 and 5.73 (each 1 H, m, H-6 and H-7). MS *m*/*z* 430 (M^+, 13), 412 (7), 394 (12), 371 (18), 55 (100). UV (EtOH) λ_{max} 272, 282, 294 nm.

20*S*,22*S*-Butyl-(1α,3*β*)-chola-5,7-diene-1,3,24-triol (17). The compound **17** was obtained from **15** (0.07 mmol) by the same procedure as described for **13** (yield 59%). ^{1}H NMR δ 0.60 (3 H, s, H-18), 0.74 (3 H, d, $J = 6.7$ Hz, H-21), 0.88 (3 H, t, $J = 7.3$ Hz, *CH*$_3$ of Bu), 0.91 (3 H, s, H-19), 3.56 and 3.72 (each 1 H, m, H-24), 3.77 (1 H, m, H-1), 4.22 (1 H, m, H-3), 5.24 and 5.59 (each 1 H, m, H-6 and H-7). MS *m*/*z* 430 (M^+, 13), 412 (7), 394 (13), 371 (20), 55 (100). UV (EtOH) λ_{max} 272, 282, 294 nm.

20*S*,22*R*-Butyl-1α,24-dihydroxy-24,25,26-trinorvitamin D$_3$ (6). The compound **6** was obtained from **18** (0.016 mmol) by the same procedure as described for **3** (yield 16%). The purity was proved to be more than 99% by two different HPLC systems: (1) YMC Pack ODS-AM 4.6 mm × 150 mm, H_2O/MeOH (15:85), 1.0 mL/min; (2) PEGASIL Silica SP100, 4.6 mm × 150 mm, hexane/$CHCl_3$/MeOH (100:25:10), 1.0 mL/min. ^{1}H NMR δ 0.53 (3 H, s, H-18), 0.74 (3 H, d, $J = 6.7$ Hz, H-21), 0.90 (3 H, t, $J = 6.7$ Hz, *CH*$_3$ of Bu), 3.62 and 3.67 (each 1 H, m, H-24), 4.23 (1 H, m, H-3), 4.43 (1 H, m, H-1), 5.00 and 5.33 (each 1 H, m, H-19), 6.02 and 6.38 (each 1 H, d, $J = 11.0$ Hz, H-7 and H-6, respectively). MS *m*/*z* 430 (M^+, 3), 412 (5), 394 (4), 134 (58), 55 (100). UV (EtOH) λ_{max} 264 nm, λ_{min} 229 nm. HRMS calcd for $C_{28}H_{46}O_3$ 430.3447, found 430.3473.

20*S*,22*S*-Butyl-1α,24-dihydroxy-24,25,26-trinorvitamin D$_3$ (5). The compound **5** was obtained from **17** (0.013 mmol) by the same procedure as described for **3** (yield 24%). The purity was proved to be more than 99% by two different HPLC systems: (1) YMC Pack ODS-AM 4.6 mm × 150 mm, H_2O/MeOH (15:85), 1.0 mL/min; (2) PEGASIL Silica SP100, 4.6 mm × 150 mm, hexane/$CHCl_3$/MeOH (100:25:10), 1.0 mL/min. ^{1}H NMR δ 0.54 (3 H, s, H-18), 0.72 (3 H, d, $J = 6.7$ Hz, H-21), 0.89 (3 H, t, $J = 6.7$ Hz, *CH*$_3$ of Bu), 3.63 and 3.72 (each 1 H, m, H-24), 4.23 (1 H, m, H-3), 4.43 (1 H, m, H-1), 5.00 and 5.33 (each 1 H, m, H-19), 6.02 and 6.38 (each 1 H, d, $J = 11.0$ Hz, H-7 and H-6, respectively). MS *m*/*z* 430 (M^+, 4), 412 (7), 394 (4), 134 (58), 55 (100). UV (EtOH) λ_{max} 264 nm, λ_{min} 228 nm. HRMS calcd for $C_{28}H_{46}O_3$ 430.3447, found 430.3434.

1α,3*β*-Bis[(methoxycarbonyl)oxy]-22*R*-butyl-5,7-choladiene-24-ol (19). To a solution of **11** (200 mg, 0.35 mmol) in THF (3 mL) was added diisobutyl-aluminum hydride (DIBAL, 1.0 M solution in toluene, 700 μL, 0.7 mmol) at −30 °C and the mixture was stirred for 1 h. Then, the mixture was allowed to 0 °C and was stirred for 3 h. The reaction mixture was poured into ice−water, extracted with ethyl acetate, washed with water, dried over Na_2SO_4, and evaporated. The residue was chromatographed on silica gel (C-200, 12 g) with 0.5% EtOH−CH_2Cl_2 to give **19** (122 mg, 64%). ^{1}H NMR δ 0.63 (3 H, s, H-18), 0.80 (3 H, d, $J = 6.9$ Hz, H-21), 0.90 (3 H, t, $J = 6.9$ Hz, *CH*$_3$ of *n*-Bu), 1.01 (3 H, s, H-19), 3.60 and 3.72 (each 1 H, m, H-24), 3.78 and 3.79 (each 3 H, s, *CH*$_3$OCO−), 4.84 (1 H, m, H-1), 4.91 (1 H, m, H-3), 5.38 and 5.69 (each 1 H, m, H-6 and H-7).

1α,3*β*-Bis[(methoxycarbonyl)oxy]-22*S*-butyl-5,7-choladiene-24-ol (20). The compound **20** was obtained from **12** (0.26 mmol) by the same procedure as described for **19** (yield 62%). ^{1}H NMR δ 0.61 (3 H, s, H-18), 0.82 (3 H, d, $J = 5.4$ Hz, H-21), 0.89 (3 H, t, $J = 6.9$ Hz, *CH*$_3$ of *n*-Bu), 1.01 (3 H, s, H-19), 3.66 (2 H, m, H-24), 3.78 and 3.79 (each 3 H, s, *CH*$_3$OCO−), 4.84 (1 H, m, H-1), 4.92 (1 H, m, H-3), 5.38 and 5.69 (each 1 H, m, H-6 and H-7). ^{13}C NMR δ 12.1, 13.5, 14.4, 16.3, 20.6, 23.1, 23.4, 28.3, 28.6, 31.0, 32.1, 35.5, 35.8, 36.6, 38.0, 38.2, 39.2, 41.4, 43.0, 53.3, 54.7, 54.9, 55.0, 62.0, 72.4, 78.6, 115.6, 122.4, 133.9, 141.4, 155.2, 155.3. MS *m*/*z* (%): 546 (M^+, 1), 470 (10), 394 (100), 251 (18), 224 (25), 209 (44), 197 (35), 167 (14), 157 (29), 149 (90), 141 (40), 129 (30), 115 (11), 105 (12). HRMS calcd for $C_{30}H_{46}O_4$ (M^+−$CH_3O(CO)OH$) 470.3396, found 470.3385. IR (neat) 3335, 2955, 2937, 2872, 1747, 1443, 1283, 1271, 1254, 1148 cm^{-1}.

1α,3*β*-Bis[(methoxycarbonyl)oxy]-22*R*-butyl-5,7-choladiene-24-al (21). To a solution of oxalyl chloride (15.5 μL, 0.18 mmol) in CH_2Cl_2 (0.8 mL) was added a solution of DMSO (27.4 μL, 0.39 mmol) in CH_2Cl_2 (0.2 mL) at −78 °C and the mixture was stirred at that temperature for 15 min. To this solution was added a solution of **19** (88 mg, 0.16 mmol) in CH_2Cl_2 (1.0 mL), and the mixture was stirred for 15 min. Triethylamine (112 μL, 0.81 mmol) was added to the reaction mixture at −78 °C, and then the mixture was allowed to warm to room temperature. The reaction mixture was diluted with CH_2Cl_2, washed with water, dried, and evaporated. The residue was chromatographed on silica gel (8 g) with 2.4% AcOEt−benzene to yield **21** (63 mg, 72%). ^{1}H NMR δ 0.64 (3 H, s, H-18), 0.82 (3 H, d, $J = 6.9$ Hz, H-21), 0.89 (3 H, t, $J = 6.9$ Hz, *CH*$_3$ of *n*-Bu), 1.01 (3 H, s, H-19), 3.78 and 3.79 (each 3 H, s, *CH*$_3$OCO−), 4.84 (1 H, m, H-1), 4.92 (1 H, m, H-3), 5.38 and 5.70 (each 1 H, m, H-6 and H-7), 9.76 (1 H, m, H-24).

1α,3*β*-Bis[(methoxycarbonyl)oxy]-22*S*-butyl-5,7-choladiene-24-al (22). The compound **22** was obtained from **20** (0.09 mmol) by the same procedure as described for **21** (yield 72%). ^{1}H NMR δ 0.59 (3 H, s, H-18), 0.82 (3 H, d, $J = 5.9$ Hz, H-21), 0.90 (3 H, t, $J = 6.9$ Hz, *CH*$_3$ of *n*-Bu), 1.01 (3 H, s, H-19), 3.78 and 3.79 (each 3 H, s, *CH*$_3$OCO−), 4.84 (1 H, m, H-1), 4.92 (1 H, m, H-3), 5.38 and 5.69 (each 1 H, m, H-6 and H-7), 9.74 (1 H, dd, $J = 2.5$, 1.5 Hz, H-24). ^{13}C NMR δ 12.0, 13.4, 14.3, 16.2, 20.6, 23.1, 23.2, 27.8, 28.0, 30.6, 32.0, 35.1, 35.7, 37.9, 39.2, 39.6, 41.4, 43.0, 47.5, 53.3, 54.7, 54.8, 55.0, 72.4, 78.6, 115.7, 122.3, 134.0, 141.1, 155.17, 155.23, 203.7. MS *m*/*z* (%): 544 (M^+, 1), 468 (10), 392 (100), 224 (24), 209 (40), 195 (13), 167 (23), 157 (22), 155 (29), 149 (45), 143 (10), 129 (12), 105 (10). HRMS calcd for $C_{30}H_{44}O_4$ (M^+−$CH_3O(CO)OH$) 468.3240, found 468.3230. IR (neat) 2955, 2858, 1744, 1441, 1271, 1252 cm^{-1}.

(1α,3*β*,22*R*,24*R*)-Bis[(methoxycarbonyl)oxy]-22-butylcholesta-5,7-dien-24-ol (23) and (1α,3*β*,22*R*,24*S*)-Bis[(methoxycarbonyl)oxy]-22-butylcholesta-5,7-dien-24-ol (24). To a solution of **21** (64 mg, 0.12 mmol) in THF (1 mL) was added isopropylmagnesium chloride (2.0 M solution in THF, 118 μL, 0.24 mmol) at room temperature and the mixture was stirred for 25 min. Then, the reaction was quenched with water. The mixture was extracted with ethyl acetate, washed with water, dried over Na_2SO_4, and evaporated. The residue was chromatographed on silica gel (C-200, 6 g) with 2−6% AcOEt−benzene to give **23** (25 mg, 36%) and **24** (29 mg, 42%) in this order. **23**: ^{1}H NMR δ 0.64 (3 H, s, H-18), 0.78 (3 H, d, $J = 6.7$ Hz, H-21), 0.90 (3 H, t, $J = 6.8$ Hz, *CH*$_3$ of *n*-Bu), 0.91 and 0.92 (each 3 H, d, $J = 6.7$ Hz, H-26 and -27), 1.02 (3 H, s, H-19), 3.35 (1 H, m, H-24), 3.77 and 3.79 (each 3 H, s, *CH*$_3$OCO−), 4.84 (1 H, m, H-1), 4.92 (1 H, m, H-3), 5.38 and 5.69 (each 1 H, m, H-6 and H-7). **24**: ^{1}H NMR δ 0.63 (3 H, s, H-18), 0.81 (3 H, d, $J = 6.7$ Hz, H-21), 0.90 (3 H, t, $J = 6.7$ Hz, *CH*$_3$ of *n*-Bu), 0.88 and 0.96 (each 3 H, d, $J = 6.7$ Hz, H-26 and -27), 1.02 (3 H, s, H-19), 3.48 (1 H, m, H-24), 3.77 and 3.79 (each 3 H, s, *CH*$_3$OCO−), 4.84 (1 H, m, H-1), 4.90 (1 H, m, H-3), 5.38 and 5.68 (each 1 H, m, H-6 and H-7).

(1α,3*β*,22*S*,24*R*)-Bis[(methoxycarbonyl)oxy]-22-butylcholesta-5,7-dien-24-ol (25) and (1α,3*β*,22*S*,24*S*)-Bis[(methoxycarbonyl)oxy]-22-butylcholesta-5,7-dien-24-ol (26). The compounds **25** (yield 34%) and **26** (yield 51%) were obtained from **22** (0.061 mmol) by the same procedure as described for **23** and **24**. **25**: ^{1}H NMR δ 0.63 (3 H, s, H-18), 0.78 (3 H, d, $J = 5.9$ Hz, H-21), 0.89 (3 H, t, $J = 6.9$ Hz, *CH*$_3$ of *n*-Bu), 0.93 (6H, d, $J = 6.4$ Hz, H-26 and -27), 1.02 (3 H, s, H-19), 3.39 (1 H, m, H-24), 3.78 and 3.79 (each 3 H, s, *CH*$_3$OCO−), 4.84 (1 H, m, H-1), 4.92 (1 H, m, H-3), 5.38 and 5.69 (each 1 H, m, H-6 and H-7). ^{13}C NMR δ 12.1, 13.2,

14.4, 16.3, 17.7, 19.0, 20.6, 23.2, 23.5, 28.4, 28.7, 30.8, 32.1, 34.6, 35.8, 36.00, 36.02, 36.9, 38.0, 39.2, 41.4, 43.1, 53.3, 54.8, 54.9, 55.1, 72.4, 74.1, 78.7, 115.7, 122.4, 133.9, 141.4, 155.2, 155.3. MS *m/z* (%): 588 (M^+, 1), 512 (5), 436 (85), 279 (15), 251 (12), 224 (23), 209 (37), 197 (27), 157 (19), 155 (28), 149 (100), 141 (26). HRMS calcd for $C_{33}H_{52}O_4$ ($M^+-CH_3O(CO)OH$) 512.3866, found 512.3861. IR (neat) 3572, 2955, 2872, 1745, 1443, 1344, 1283, 1254, 1148 cm^{-1}. **26**: ^1H NMR δ 0.61 (3 H, s, H-18), 0.83 (3 H, d, $J = 6.4$ Hz, H-21), 0.90 (3 H, t, $J = 6.9$ Hz, CH_3 of *n*-Bu), 0.89 and 0.95 (each 3 H, d, $J = 6.9$ Hz, H-26 and -27), 1.01 (3 H, s, H-19), 3.45 (1 H, m, H-24), 3.78 and 3.79 (each 3 H, s, CH_3OCO-), 4.84 (1 H, m, H-1), 4.92 (1 H, m, H-3), 5.38 and 5.69 (each 1 H, m, H-6 and H-7). ^{13}C NMR δ 12.1, 13.7, 14.4, 16.2, 16.3, 19.5, 20.6, 23.2, 23.5, 28.2, 29.1, 31.3, 32.1, 33.2, 35.8, 37.5, 38.0, 38.3, 39.2, 39.7, 41.4, 43.0, 53.6, 54.7, 54.8, 55.0, 72.4, 76.1, 78.7, 115.6, 122.4, 133.9, 141.4, 155.2, 155.3. MS *m/z* (%): 588 (M^+, 1), 512 (10), 436 (100), 251 (14), 249 (12), 223 (13), 210 (16), 197 (34), 183 (13), 157 (24), 155 (35), 143 (11), 141 (32), 129 (14). HRMS calcd for $C_{33}H_{52}O_4$ ($M^+-CH_3O(CO)OH$) 512.3866, found 512.3862. IR (neat) 3695, 2957, 2872, 1745, 1443, 1281, 1271, 1252 cm^{-1}.

(1α,3β,22*R*,24*R*)-22-butylcholesta-5,7-diene-1,3,24-triol (27). To a solution of **23** (28 mg, 0.048 mmol) in CH_2Cl_2 (0.6 mL) was added 5% KOH/MeOH (3.4 mL) and the mixture was stirred at 40 °C for 1.5 h. The reaction mixture was diluted with $CHCl_3$, washed with water, dried over Na_2SO_4, and evaporated. The residue was chromatographed on silica gel with 65% AcOEt−CH_2Cl_2 to give **27** (18 mg, 80%). ^1H NMR δ 0.65 (3 H, s, H-18), 0.80 (3 H, d, $J = 6.7$ Hz, H-21), 0.91 (3 H, t, $J = 6.7$ Hz, CH_3 of *n*-Bu), 0.91 and 0.93 (each 3 H, d, $J = 6.7$ Hz, H-26 and -27), 0.95 (3 H, s, H-19), 3.34 (1 H, m, H-24), 3.77 (1 H, m, H-1), 4.10 (1 H, m, H-3), 5.38 and 5.73 (each 1 H, m, H-6 and H-7). MS *m/z* 472 (M^+, 13), 454 (9), 436 (13), 413 (14), 55 (100). UV (EtOH) λ_{max} 272, 282, 294 nm.

Compounds 28−30. By the same procedure as described for **27**, each triol **28** (yield 57%), **29** (yield 60%), and **30** (yield 57%) was obtained from the corresponding precursors, **24** (0.043 mmol), **25** (0.026 mmol), and **26** (0.036 mmol), respectively.

(1α,3β,22*R*,24*S*)-22-butylcholesta-5,7-diene-1,3,24-triol (28). ^1H NMR δ 0.65 (3 H, s, H-18), 0.82 (3 H, d, $J = 6.7$ Hz, H-21), 0.90 (3 H, t, $J = 7.3$ Hz, CH_3 of *n*-Bu), 0.88 and 0.96 (each 3 H, d, $J = 6.7$ Hz, H-26 and -27), 0.95 (3 H, s, H-19), 3.49 (1 H, m, H-24), 3.77 (1 H, m, H-1), 4.09 (1 H, m, H-3), 5.38 and 5.73 (each 1 H, m, H-6 and H-7). MS *m/z* 472 (M^+, 14), 454 (10), 436 (15), 413 (19), 55 (100). UV (EtOH) λ_{max} 272, 282, 294 nm.

(1α,3β,22*S*,24*R*)-22-butylcholesta-5,7-diene-1,3,24-triol (29). ^1H NMR δ 0.64 (3 H, s, H-18), 0.80 (3 H, d, $J = 5.9$ Hz, H-21), 0.90 (3 H, t, $J = 6.7$ Hz, CH_3 of *n*-Bu), 0.93 (6 H, d, $J = 6.7$ Hz, H-26 and -27), 0.96 (3 H, s, H-19), 3.40 (1 H, m, H-24), 3.78 (1 H, m, H-1), 4.08 (1 H, m, H-3), 5.39 and 5.74 (each 1 H, m, H-6 and H-7). MS *m/z* 472 (M^+, 27), 454 (16), 436 (21), 413 (21), 55 (100). UV (EtOH) λ_{max} 272, 282, 294 nm.

(1α,3β,22*S*,24*S*)-22-butylcholesta-5,7-diene-1,3,24-triol (30). ^1H NMR δ 0.63 (3 H, s, H-18), 0.85 (3 H, d, $J = 6.7$ Hz, H-21), 0.90 (3 H, t, $J = 6.7$ Hz, CH_3 of *n*-Bu), 0.89 and 0.95 (each 3 H, d, $J = 6.7$ Hz, H-26 and -27), 0.95 (3 H, s, H-19), 3.46 (1 H, m, H-24), 3.77 (1 H, m, H-1), 4.07 (1 H, m, H-3), 5.39 and 5.73 (each 1 H, m, H-6 and H-7). MS *m/z* 472 (M^+, 15), 454 (11), 436 (17), 413 (19), 55 (100). UV (EtOH) λ_{max} 272, 282, 294 nm.

Compounds 7−10. By the same procedure as described for **3**, compounds **7** (yield 21%), **8** (yield 26%), **9** (yield 28%), and **10** (yield 27%) were obtained from the corresponding precursors, **27** (0.01 mmol), **28** (0.016 mmol), **29** (0.017 mmol), and **30** (0.011 mmol), respectively. The purity of compounds **7−10** was proved to be more than 99% by two different HPLC systems: (1) YMC Pack ODS-AM 4.6 mm × 150 mm, H_2O/MeOH (10:90), 1.0 mL/min; (2) PEGASIL Silica SP100, 4.6 mm × 150 mm, hexane/$CHCl_3$/MeOH (100:25:8), 1.0 mL/min.

(1α,22*R*,24*R*)-22-Butyl-1,24-dihydroxyvitamin D_3 (7). ^1H NMR δ 0.58 (3 H, s, H-18), 0.77 (3 H, d, $J = 6.7$ Hz, H-21), 0.90 (3 H, t, $J = 6.7$ Hz, CH_3 of *n*-Bu), 0.91 and 0.93 (each 3 H, d, $J = 6.7$ Hz, H-26 and -27), 3.35 (1 H, m, H-24), 4.23 (1 H, m, H-3), 4.43 (1 H, m, H-1), 5.01 and 5.33 (each 1 H, m, H-19), 6.02 and 6.38 (each 1 H, d, $J = 11.0$ Hz, H-7 and H-6, respectively). MS *m/z* 472 (M^+, 3), 454 (9), 436 (6), 152 (22),134 (72), 55 (100). UV (EtOH) λ_{max} 264 nm, λ_{min} 229 nm. HRMS calcd for $C_{31}H_{52}O_3$ 472.3916, found 472.3904.

(1α,22*R*,24*S*)-22-Butyl-1,24-dihydroxyvitamin D_3 (8). ^1H NMR δ 0.57 (3 H, s, H-18), 0.80 (3 H, d, $J = 6.8$ Hz, H-21), 0.89 (3 H, t, $J = 6.7$ Hz, CH_3 of *n*-Bu), 0.89 and 0.97 (each 3 H, d, $J = 6.7$ Hz, H-26 and -27), 3.49 (1 H, m, H-24), 4.23 (1 H, m, H-3), 4.43 (1 H, m, H-1), 5.00 and 5.33 (each 1 H, m, H-19), 6.02 and 6.38 (each 1 H, d, $J = 11.0$ Hz, H-7 and H-6, respectively). MS *m/z* 472 (M^+, 3), 454 (11), 436 (11), 152 (21),134 (77), 55 (100). UV (EtOH) λ_{max} 264 nm, λ_{min} 229 nm. HRMS calcd for $C_{31}H_{52}O_3$ 472.3916, found 472.3942.

(1α,22*S*,24*R*)-22-Butyl-1,24-dihydroxyvitamin D_3 (9). ^1H NMR δ 0.57 (3 H, s, H-18), 0.78 (3 H, d, $J = 5.5$ Hz, H-21), 0.90 (3 H, t, $J = 6.7$ Hz, CH_3 of *n*-Bu), 0.92 (6 H, d, $J = 6.7$ Hz, H-26 and −27), 3.38 (1 H, m, H-24), 4.23 (1 H, m, H-3), 4.43 (1 H, m, H-1), 5.00 and 5.33 (each 1 H, s, m, H-19), 6.02 and 6.38 (each 1 H, d, $J = 11.0$ Hz, H-7, H-6, respectively. MS *m/z* 472 (M^+, 4), 454 (9), 436 (6), 152 (23),134 (76), 55 (100). UV (EtOH) λ_{max} 265 nm, λ_{min} 228 nm. HRMS calcd for $C_{31}H_{52}O_3$ 472.3916, found 472.3893.

(1α,22*S*,24*S*)-22-Butyl-1,24-dihydroxyvitamin D_3 (10). ^1H NMR δ 0.55 (3 H, s, H-18), 0.83 (3 H, d, $J = 5.4$ Hz, H-21), 0.90 (3 H, t, $J = 7.4$ Hz, CH_3 of *n*-Bu), 0.89 and 0.95 (each 3 H, d, $J = 6.7$ Hz, H-26 and -27), 3.45 (1 H, m, H-24), 4.23 (1 H, m, H-3), 4.43 (1 H, m, H-1), 5.01 and 5.33 (each 1 H, m, H-19), 6.02 and 6.38 (each 1 H, d, $J = 11.0$ Hz, H-7 and H-6, respectively). MS *m/z* 472 (M^+, 3), 454 (9), 436 (5), 152 (22),134 (76), 55 (100). UV (EtOH) λ_{max} 265 nm, λ_{min} 229 nm. HRMS calcd for $C_{31}H_{52}O_3$ 472.3916, found 472.3893.

(3*R*,5*R*)-5-(1-{(1*S*,3*R*,10*R*,13*R*,17*R*)-1,3-bis[(methoxycarbonyl)oxy]-10,13-dimethyl-2,3,4,9,10,11,12,13,14,15,16,17-dodecahydro-1*H*-cyclopenta[a]phenanthren-17-yl}ethyl)-2-methylnonan-3-yl (2*S*)-3,3,3-Trifluoro-2-methoxy-2-phenylpropanoate (31). To a solution of compound **23** (6.1 mg, 0.010 mmol) in dry CH_2Cl_2 (100 μL) were added Et_3N (30 μL, 0.21 mmol), a solution of *R*-MTPACl (20 μL, 0.10 mmol) in dry CH_2Cl_2 (60 μL), and DMAP (15.5 mg, 0.13 mmol), and the reaction mixture was stirred for 30 min at room temperature. The reaction was quenched with H_2O at 0 °C and was extracted with AcOEt. The organic layer was washed with brine, dried over $MgSO_4$, and evaporated. The residue was chromatographed on silica gel (5 g, hexane/AcOEt = 4/1) to give *S*-MTPA ester **31** (5.8 mg, 69.6%). **31**: ^1H NMR δ 0.57 (3 H, s, H-18), 0.76 (3 H, d, $J = 6.7$ Hz, H-21), 0.84 and 0.89 (each 3 H, d, $J = 6.9$ Hz, H-26, 27), 0.90 (3 H, t, $J = 7.2$ Hz, CH_3 of Bu), 1.01 (3 H, s, H-19), 3.49 (3 H, s, OCH_3), 3.776 and 3.784 (each 3 H, s, $O(CO)OCH_3$), 4.84 (1 H, m, H-1), 4.90 (1 H, m, H-3), 5.08 (1 H, dd, $J = 10.3$, 1.7 Hz, H-24), 5.36 (1 H, dd, $J = 5.6$, 2.9 Hz, H-7), 5.69 (1 H, dd, $J = 5.6$, 1.9 Hz, H-6), 7.40 (3 H, m, Ph-3, 4, 5), 7.53 (2 H, m, Ph-2, 6).

(3*R*,5*R*)-5-(1-{(1*S*,3*R*,10*R*,13*R*,17*R*)-1,3-bis[(methoxycarbonyl)oxy]-10,13-dimethyl-2,3,4,9,10,11,12,13,14,15,16,17-dodecahydro-1*H*-cyclopenta[a]phenanthren-17-yl}ethyl)-2-methylnonan-3-yl (2*R*)-3,3,3-Trifluoro-2-methoxy-2-phenylpropanoate (32). In a similar manner to that for the synthesis of **31** from **23**, a crude product was obtained from **23** (14.4 mg, 0.024 mmol), Et_3N (36 μL, 0.24 mmol), *S*-MTPACl (23 μL, 0.24 mmol), and DMAP (18.7 mg, 0.15 mmol) in dry CH_2Cl_2 at room temperature for 30 min and was purified by chromatographed on silica gel (5 g, hexane/AcOEt = 4/1) to give *R*-MTPA ester **32** (5.8 mg, 29.5%). **32**: ^1H NMR δ 0.53 (3 H, s, H-18), 0.72 (3 H, d, $J = 6.7$ Hz, H-21), 0.92 (3 H, t, $J = 7.1$ Hz, CH_3 of Bu), 0.93 (6 H, d, $J = 6.9$ Hz, H-26, 27), 1.00 (3 H, s, H-19), 3.58 (3 H, s, OCH_3), 3.776 and 3.779 (each 3 H, s, $O(CO)OCH_3$), 4.83 (1 H, m, H-1), 4.89 (1 H, m, H-3), 5.09 (1 H, dd, $J = 9.6$, 3.7 Hz, H-24), 5.35 (1 H, dd, $J = 5.6$, 2.9 Hz, H-7), 5.69 (1 H, dd, $J = 5.6$, 1.8 Hz, H-6), 7.39 (3 H, m, Ph-3, 4, 5), 7.55 (2 H, m, Ph-2, 6).

(3*S*,5*S*)-5-(1-{(1*S*,3*R*,10*R*,13*R*,17*R*)-1,3-bis[(methoxycarbonyl)oxy]-10,13-dimethyl-2,3,4,9,10,11,12,13,14,15,16,17-dodecahydro-1*H*-cyclopenta[a]phenanthren-17-yl}ethyl)-2-methylnonan-3-yl (2*S*)-3,3,3-Trifluoro-2-methoxy-2-phenylpropanoate (33). Compound **33** was obtained from **26** (0.01 mmol) by the same procedure as described for **31** (yield 97.1%). **33**: ^{1}H NMR δ 0.59 (3 H, s, H-18), 0.83 (3 H, d, J = 6.1 Hz, H-21), 0.90 (3 H, t, J = 6.8 Hz, CH_3 of Bu), 0.91 and 0.93 (each 3 H, d, J = 6.9 Hz, H-26, 27), 1.01 (3 H, s, H-19), 3.53 (3 H, s, OCH_3), 3.78 and 3.79 (each 3 H, s, O(CO)OCH_3), 4.85 (1 H, m, H-1), 4.90 (1 H, m, H-3), 5.04 (1 H, m, H-24), 5.37 (1 H, m, H-7), 5.69 (1 H, dd, J = 5.6, 2.0 Hz, H-6), 7.39 (3 H, m, Ph-3, 4, 5), 7.54 (2 H, m, Ph-2, 6).

(3*S*,5*S*)-5-(1-{(1*S*,3*R*,10*R*,13*R*,17*R*)-1,3-bis[(methoxycarbonyl)oxy]-10,13-dimethyl-2,3,4,9,10,11,12,13,14,15,16,17-dodecahydro-1*H*-cyclopenta[*a*]phenanthren-17-yl}ethyl)-2-methylnonan-3-yl (2*R*)-3,3,3-trifluoro-2-methoxy-2-phenylpropanoate (34). Compound **34** was obtained from **26** (0.01 mmol) by the same procedure as described for **32** (yield 93.1%). **34**: ^{1}H NMR δ 0.61 (3 H, s, H-18), 0.83 (3 H, d, J = 6.8 Hz, H-21), 0.85 and 0.88 (each 3 H, d, J = 6.7 Hz, H-26, 27), 0.90 (3 H, t, J = 6.8 Hz, CH_3 of Bu), 1.01 (3 H, s, H-19), 3.56 (3 H, s, OCH_3), 3.78 and 3.79 (each 3 H, s, O(CO)OCH_3), 4.84 (1 H, m, H-1), 4.91 (1 H, m, H-3), 5.05 (1 H, m, H-24), 5.37 (1 H, m, H-7), 5.69 (1 H, dd, J = 5.6, 1.9 Hz, H-6), 7.40 (3 H, m, Ph-3, 4, 5), 7.56 (2 H, m, Ph-2, 6).

Competitive Binding Assay, Bovine Thymus VDR. Binding to bovine thymus VDR was evaluated according to the procedure reported.[20] Bovine thymus VDR was purchased from Yamasa Biochemical (Choshi, Chiba, Japan) and dissolved in 0.05 M phosphate buffer (pH 7.4) containing 0.3 M KCl and 5 mM dithiothreitol just before use. The receptor solution (500 μL) in an assay tube was incubated with 0.072 nM [^{3}H]-1,25-$(OH)_2D_3$ together with graded amounts of each vitamin D analogue (0.001−20 nM) or vehicle for 19 h at 4 °C. The bound and free [^{3}H]-1,25-$(OH)_2D_3$ were separated by treating with dextran-coated charcoal for 20 min at 4 °C. The assay tubes were centrifuged at 1000*g* for 10 min. The radioactivity of the supernatant was counted. Nonspecific binding was subtracted. These experiments were done in duplicate.

Transfection and Transactivation Assay. COS-7 cells were cultured in Dulbecco's modified Eagle's medium (DMEM) supplemented with 5% fetal bovine serum (FBS). Cells were seeded on 24-well plates at a density of 2×10^4 per well. After 24 h, the cells were transfected with a reporter plasmid containing three copies of the mouse osteopontin VDRE (5′-GGTTCAcgaGGTTCA, SPPx3-TK-Luc), a wild-type or mutant hVDR expression plasmid (pCMX-hVDR), and the internal control plasmid containing sea pansy luciferase expression constructs (pRL-CMV) by the lipofection method as described previously.[32] After 8 h of incubation, the cells were treated with either the ligand or ethanol vehicle and cultured for 16 h. Cells in each well were harvested with a cell lysis buffer, and the luciferase activity was measured with a luciferase assay kit (Promega, Wisconsin). Transactivation measured by the luciferase activity was normalized with the internal control. All experiments were done in triplicate.

Quantitative Real-Time RT-PCR Analysis. Total RNAs from samples were prepared with RNAgents Total RNA Isolation system (Promega), and cDNAs were synthesized using the ImProm-II reverse transcription system (Promega). Real-time PCR was performed on the ABI PRISM 7300 sequence detection system (Applied Biosystems, Foster City, CA) using SYBR Green Realtime PCR Master Mix -Plus- (Toyobo, Osaka, Japan). Primers were as follows: CYP24A1, 5′-TGA ACG TTG GCT TCA GGA GAA-3′ and 5′-AGG GTG CCT GAG TGT AGC ATC T-3′; actin, 5′-GAC AGG ATG CAG AAG GAG AT-3′ and 5′-GAA GCA TTT GCG GTG GAC GAT-3′. The RNA values were normalized to the level of Actin mRNA and represent the mean ± SD of triplicate assays.

Differentiation of HL-60 Cells. Human promyelocytic leukemia cells (HL-60) were plated at 2×10^5 cells/plate and were cultured in Eagle's modified medium as described previously.[33] The cells were incubated with each vitamin D compound (10^{-6}, 10^{-7} and 10^{-8} M) for 4 days. The differentiation activity was determined by an NBT reduction assay method as previously reported.[33,34] The experiments were done in duplicate.

X-ray Crystallographic Analysis of the Complex Structure. In this study, the method reported by Vanhooke et al.[6] was used with some modifications to prepare the crystals of VDR complexes. The rat VDR−LBD (residues 116−423, Δ165−211) was cloned as an N-terminal His_6-tagged fusion protein into the pET14b expression vector and overproduced in *Escherichia coli* C41. The cells were grown at 37 °C in LB medium (including ampicilin 100 mg/L) and subsequently induced for 6 h with 15 μM isopropyl-β-D-thiogalactopyranoside (IPTG) at 23 °C. The purification procedure included affinity chromatography on a Ni-NTA column, followed by dialysis and cation-exchange chromatography (SP-Sepharose). After tag removal by thrombin digestion, protease was removed by filtration through a HiTrap benzamidine column and the protein was further purified by gel filtration on a Superdex200 column. The purity and homogeneity of the rVDR−LBD were assessed by SDS-PAGE.

Purified rVDR−LBD solution was concentrated to about 0.75 mg/mL by ultrafiltration. To an aliquot (800 μL) of the protein solution was added a ligand (ca. 10 equiv), the solution was further concentrated to about 1/8, and then a solution (25 mM Tris-HCl, pH 8.0; 50 mM NaCl; 10 mM DTT; 0.02% NaN_3) of coactivator peptide (H_2N-KNHPMLMNLLKDN-$CONH_2$) derived from DRIP205 was added. This solution of VDR/ligand/peptide was allowed to crystallize by the vapor diffusion method using a series of precipitant solutions containing 0.1 M MOPS−NaOH (pH7.0), 0.1−0.4 M sodium formate, 12−22% (w/v) PEG4000, and 5% (v/v) ethylene glycol. Droplets for crystallization were prepared by mixing 2 μL of complex solution and 1 μL precipitant solution, and droplets were equilibrated against 500 μL precipitant solution at 20 °C. It took 1−2 days to obtain reproducible crystals with X-ray diffraction quality for VDR complex with the ligand **5**. On the other hand, the VDR complex with the ligand **4** gave only crystals of poor quality except the one used for the structure determination, which was barely suitable for X-ray diffraction experiment.

Prior to diffraction data collection, crystals were soaked in a cryoprotectant solution containing 0.1 M MOPS−NaOH (pH 7.0), 0.1−0.4 M sodium formate, 15−20% PEG4000, and 17−20% ethylene glycol. Diffraction data sets were collected at 100 K in a stream of nitrogen gas at beamline BL-6A of KEK-PF (Tsukuba, Japan). Reflections were recorded with an oscillation range per image of 1.0°. Diffraction data were indexed, integrated, and scaled using the program HKL2000.[35] The structures of complex were solved by molecular replacement with the program CNS[36] using a rat VDR−LBD coordinates (PDB code: 1RK3), and finalized sets of atomic coordinates were obtained after iterative rounds of model modification with the program XtalView[37] and refinement with CNS by rigid body refinement, simulated annealing, positional minimization, water molecule identification, and individual isotropic B-value refinement. The coordinates of the two complexes were deposited in the Protein Data Bank with accession number 2ZXM for ligand **4** and 2ZXN for ligand **5**.

Graphical Manipulations and Ligand Docking. Graphical manipulations were performed using SYBYL 8.0 (Tripos, St. Louis). The atomic coordinates of the crystal structure of zVDR-LBD complexed with GEMINI (**1b**) were retrieved from Protein Data Bank (PDB) (entry 2HCD).[11] 22-Butyl vitamin D analogues (**3**, **6**, **7**−**10**) were docked into the ligand-binding pocket using Surflex Dock 2.0 (Tripos, St. Louis), and then the docking models were modified to agree with the biological activities.

Acknowledgment. Part of this work was supported by a Grant-in-Aid for Scientific Research (no. 20590108) from the Ministry of Education, Culture, Sports, Science, and Technology, Japan.

Supporting Information Available: Transcriptional activities in HEK293 cells, ASMA, recruitment of RXR and SRC-1, and

HPLC charts to prove purity of compounds **3**−**10**. This material is available free of charge via the Internet at http://pubs.acs.org.

References

(1) Feldman, D.; Pike, J. W. Glorieux, F. H. , Eds. *Vitamin D*, 2nd ed.; Elsevier Academic Press: New York, 2005.

(2) Jurutka, P. W.; Whitfield, G. K.; Hsieh, J. C.; Thompson, P. D.; Haussler, C. A.; Haussler, M. R. Synthesis and Conformational Analysis of 17α,21-Cyclo-22-Unsaturated Analogues of Calcitriol. *Rev. Endocr. Metab. Disord.* **2001**, *2*, 203–216.

(3) Yamada, S.; Shimizu, M.; Yamamoto, K. Vitamin D Receptor. In *Vitamin D and Rickets, Endocrine Development*, Vol. 6; Hochberg, Z., Ed.; Karger: Basel, Switzerland, 2003; pp 50−68.

(4) Rochel, N.; Wurtz, J. M.; Mitschler, A.; Klaholz, B.; Moras, D. The Crystal Structure of the Nuclear Receptor for Vitamin D Bound to Its Natural Ligand. *Mol. Cell* **2000**, *5*, 173–179.

(5) Tocchini-Valentini, G.; Rochel, N.; Wurtz, J. M.; Mitschler, A.; Moras, D. Crystal structures of the vitamin D receptor complexed to super agonist 20-epi ligands. *Proc. Natl. Acad. Sci. U.S.A.* **2001**, *98*, 5491–5496.

(6) Vanhooke, J. L.; Benning, M. M.; Bauer, C. B.; Pike, J. W.; DeLuca, H. F. Molecular Structure of the Rat Vitamin D Receptor Ligand Binding Domain Complexed with 2-Carbon-Substituted Vitamin D_3 Hormone Analogues and a LXXLL-Containing Coactivator Peptide. *Biochemistry* **2004**, *43*, 4101–4110.

(7) Ciesielski, F.; Rochel, N.; Mitschler, A.; Kouzmenko, A.; Moras, D. Structural investigation of the ligand binding domain of the zebrafish VDR in complexes with 1 α,25$(OH)_2D_3$ and Gemini: purification, crystallization and preliminary X-ray diffraction analysis. *J. Steroid Biochem. Mol. Biol.* **2004**, *89*−*90*, 55–59.

(8) Tocchini-Valentini, G.; Rochel, N.; Wurtz, J.-M.; Moras, D. Crystal Structures of the Vitamin D Nuclear Receptor Liganded with the Vitamin D Side Chain Analogues Calcipotriol and Seocalcitol, Receptor Agonists of Clinical Importance. Insights into a Structural Basis for the Switching of Calcipotriol to a Receptor Antagonist by Further Side Chain Modification. *J. Med. Chem.* **2004**, *47*, 1956–1961.

(9) Eelen, G.; Verlinden, L.; Rochel, N.; Claessens, F.; De Clercq, P.; Vandewalle, M.; Tocchini-Valentini, G.; Moras, D.; Bouillon, R.; Verstuyf, A. Superagonistic action of 14-epi-analogs of 1,25-dihydroxyvitamin D explained by vitamin D receptor−coactivator interaction. *Mol. Pharmacol.* **2005**, *67*, 1566–73.

(10) Hourai, S.; Fujishima, T.; Kittaka, A.; Suhara, Y.; Takayama, H.; Rochel, N.; Moras, D. Probing a water channel near the A-ring of receptor-bound 1α,25-dihydroxyvitamin D_3 with selected 2α-substituted analogues. *J. Med. Chem.* **2006**, *49*, 5199–5205.

(11) Ciesielski, F.; Rochel, N.; Moras, D. Adaptability of the Vitamin D nuclear receptor to the synthetic ligand Gemini: remodelling the LBP with one side chain rotation. *J. Steroid Biochem. Mol. Biol.* **2007**, *103*, 235–42.

(12) Rochel, N.; Hourai, S.; Perez-Garcia, X.; Rumbo, A.; Mourino, A.; Moras, D. Crystal structure of the vitamin D nuclear receptor ligand binding domain in complex with a locked side chain analog of calcitriol. *Arch. Biochem. Biophys.* **2007**, *460*, 172–176.

(13) Vanhooke, J. L.; Tadi, B. P.; Benning, M. M.; Plum, L. A.; DeLuca, H. F. New analogs of 2-methylene-19-nor-(20*S*)-1,25-dihydroxyvitamin D_3 with conformationally restricted side chains: evaluation of biological activity and structural determination of VDR-bound conformations. *Arch. Biochem. Biophys.* **2007**, *460*, 161–165.

(14) Hourai, S.; Rodrigues, L. C.; Antony, P.; Reina-San-Martin, B.; Ciesielski, F.; Magnier, B. C.; Schoonjans, K.; Mourino, A.; Rochel, N.; Moras, D. Structure-based design of a superagonist ligand for the vitamin D nuclear receptor. *Chem. Biol.* **2008**, *15*, 383–392.

(15) Shimizu, M.; Miyamoto, Y.; Takaku, H.; Matsuo, M.; Nakabayashi, M.; Masuno, H.; Udagawa, N.; DeLuca, H. F.; Ikura, T.; Ito, N. 2-Substituted-16-ene-22-thia-1α,25-dihydroxy-26,27-dimethyl-19-norvitamin D_3 analogs: Synthesis, biological evaluation, and crystal structure. *Bioorg. Med. Chem.* **2008**, *16*, 6949–6964.

(16) Nakabayashi, M.; Yamada, S.; Yoshimoto, N.; Tanaka, T.; Igarashi, M.; Ikura, T.; Ito, N.; Makishima, M.; Tokiwa, H.; Deluca, H. F.; Shimizu, M. Crystal Structures of Rat Vitamin D Receptor Bound to Adamantyl Vitamin D Analogs: Structural Basis for Vitamin D Receptor Antagonism and Partial Agonism. *J. Med. Chem.* **2008**, *51*, 5320–5329.

(17) Uskokovic, M. R.; Manchand, P. S.; Peleg, S.; Norman, A. W. Synthesis and preliminary evaluation of the biological properties of a 1α,25-dihydroxyvitamin D3 analogue with two side chains. In *Vitamin D: Chemistry, Biology and Clinical Applications of the Steroid Hormone*; Norman, A. W., Bouillon, R., Thomasset, M., Eds.; University of California: Riverside, 1997; pp19−21.

(18) Kurek-Tyrlik, A.; Makaev, F. Z.; Wicha, J.; Zhabinskii, V.; Calverley, M. J. Pivoting 20-Normal and 20-Epi Calcitriols: Synthesis and Crystal Structure of a "Double Side Chain" Analogue. In *Vitamin D: Chemistry, Biology and Clinical Applications of the Steroid Hormone*; Norman, A. W., Bouillon, R., Thomasset, M., Eds.; University of California: Riverside, 1997; pp30−31.

(19) Norman, A. W.; Manchand, P. S.; Uskokovic, M. R.; Okamura, W. H.; Takeuchi, J. A.; Bishop, J. E.; Hisatake, J. I.; Koeffler, H. P.; Peleg, S. Characterization of a novel analogue of 1α,25$(OH)_2$-vitamin D_3 with two side chains: interaction with its nuclear receptor and cellular actions. *J. Med. Chem.* **2000**, *43*, 2719–2730.

(20) Yamamoto, K.; Sun, W.-Y.; Ohta, M.; Hamada, K.; DeLuca, H. F.; Yamada, S. Conformationally Restricted Analogs of 1α,25-Dihydroxyvitamin D_3 and Its 20-Epimer: Compounds for Study of the Three-Dimensional Structure of Vitamin D Responsible for Binding to the Receptor. *J. Med. Chem.* **1996**, *39*, 2727–2737.

(21) Yamamoto, K.; Ooizumi, H.; Umesono, K.; Verstuyf, A.; Bouillon, R.; DeLuca, H. F.; Shinki, T.; Suda, T.; Yamada, S. Three-dimensional structure-function relationship of vitamin D: side chain location and various activities. *Bioorg. Med. Chem. Lett.* **1999**, *9*, 1041–1046.

(22) Yamamoto, K.; Inaba, Y.; Yoshimoto, N.; Choi, M.; DeLuca, H. F.; Yamada, S. 22-Alkyl-20-epi-1α,25-dihydroxyvitamin D_3 Compounds of Super-agonistic Activity: Syntheses, Biological Activities and Interaction with the Receptor. *J. Med. Chem.* **2007**, *50*, 932–939.

(23) Yoshimoto, N.; Inaba, Y.; Yamada, S.; Makishima, M.; Shimizu, M.; Yamamoto, K. 2-Methylene 19-nor-25-dehydro-1α-hydroxyvitamin D_3 26,23-lactones: Synthesis, biological activities and molecular basis of passive antagonism. *Bioorg. Med. Chem.* **2008**, *16*, 457–473.

(24) Yamamoto, K.; Ogura, H.; Jukuta, J.; Inoue, H.; Hamada, K.; Sugiyama, Y.; Yamada, S. Stereochemical and Mechanistic Studies on Conjugate Addition of Organocuprates to Acyclic Enones and Enoates: Simple Rule for Diastereofacial Selectivity. *J. Org. Chem.* **1998**, *63*, 4449–4458.

(25) Ohtani, I.; Kusumi, T.; Kashman, Y.; Kakisawa, H. *J. Am. Chem. Soc.* **1991**, *113*, 4092.

(26) GenBank accession no. Q28037.

(27) GenBank accession no. P11473.

(28) Peleg, S.; Liu, Y. Y.; Reddy, S.; Horst, R. L.; White, M. C.; Posner, G. H. A 20-epi side chain restores growth-regulatory and transcriptional activities of an A ring-modified hybrid analog of 1α,25-dihydroxyvitamin D_3 without increasing its affinity to the vitamin D receptor. *J. Cell. Biochem.* **1996**, *63*, 149–161.

(29) (a) Haussler, M. R.; Whitfield, G. K.; Haussler, C. A.; Hsieh, J. C.; Thompson, P. D.; Selznick, S. H.; Dominguez, C. E.; Jurutka, P. W. The nuclear vitamin D receptor: biological and molecular regulatory properties revealed. *J. Bone Miner. Res.* **1998**, *13*, 325–349. (b) Abe, E.; Miyaura, C.; Sakagami, H. I.; Takeda, M; Konno, K.; Yamazaki, T.; Yoshiki, S.; Suda, T. Differentiation of mouse myeloid leukemia cells induced by 1α,25-dihydroxyvitamin D_3. *Proc. Natl. Acad. Sci. U.S.A.* **1981**, *78*, 4990–4994.

(30) Yamamoto, K.; Abe, D.; Yoshimoto, N.; Choi, M.; Yamagishi, K.; Tokiwa, H.; Shimizu, M.; Makishima, M.; Yamada, S. Vitamin D Receptor: Ligand Recognition and Allosteric Network. *J. Med. Chem.* **2006**, *49*, 1313–1324.

(31) Inaba, Y.; Yamamoto, K.; Yoshimoto, N.; Matsunawa, M.; Uno, S.; Yamada, S.; Makishima, M. Vitamin D_3 derivatives with adamantane or lactone ring side chains are cell type-selective vitamin D receptor modulators. *Mol. Pharmacol.* **2007**, *71*, 1298.

(32) Yamamoto, K.; Masuno, H.; Choi, M.; Nakashima, K.; Taga, T.; Ooizumi, H.; Umesono, K.; Sicinska, W.; Van Hooke, J.; DeLuca, H. F.; Yamada, S. Three-dimensional modeling of and ligand docking to vitamin D receptor ligand binding domain. *Proc. Natl. Acad. Sci. U.S.A.* **2000**, *97*, 1467–1472.

(33) Sicinski, R. R.; Prahl, J. M.; Smith, C. M.; DeLuca, H. F. New 1α,25-dihydroxy-19-norvitamin D_3 compounds of high biological activity: Synthesis and biological evaluation of 2-hydroxymethyl, 2-methyl, and 2-methylene analogues. *J. Med. Chem.* **1998**, *41*, 4662–4674.

(34) Sicinski, R. R.; Perlman, K. L.; Prahl, J.; Smith, C.; DeLuca, H. F. Synthesis and biological activity of 1α,25-dihydroxy-18-norvitamin D_3 and 1α,25-dihydroxy-18,19-dinorvitamin D_3. *J. Med. Chem.* **1996**, *39*, 4497–4506.

(35) Otwinowski, Z.; Minor, W. Processing of X-ray diffraction data collected in oscillation mode. *Methods Enzymol.* **1997**, *276*, 307–326.

(36) Brünger, A. T.; Adams, P. D.; Clore, G. M.; DeLano, W. L.; Gros, P.; Grosse-Kunstleve, R. W.; Jiang, J.-S.; Kuszewski, J.; Nilges, M.; Pannu, N. S.; Read, R. J.; Rice, L. M.; Simonson, T.; Warren, G. L. Crystallography & NMR system: a new software suite for macromolecular structure determination. *Acta Crystallogr., Sect. D: Biol. Crystallogr.* **1998**, *54*, 905–921.

(37) McRee, D. E. XtalView/Xfits a versatile program for manipulating atomic coordinates and electron density. *J. Struct. Biol.* **1999**, *125*, 156–165.

JM8014348